Published for SISSA by Springer

Received: December 13, 2022
Accepted: April 2, 2023
Published: July 27, 2023

Search for long-lived particles using out-of-time trackless jets in proton-proton collisions at $\sqrt{s} = 13$ TeV

The CMS collaboration

E-mail: cms-publication-committee-chair@cern.ch

Abstract: A search for long-lived particles decaying in the outer regions of the CMS silicon tracker or in the calorimeters is presented. The search is based on a data sample of proton-proton collisions at $\sqrt{s} = 13$ TeV recorded with the CMS detector at the LHC in 2016–2018, corresponding to an integrated luminosity of 138 fb^{-1}. A novel technique, using nearly trackless and out-of-time jet information combined in a deep neural network discriminator, is employed to identify decays of long-lived particles. The results are interpreted in a simplified model of chargino-neutralino production, where the neutralino is the next-to-lightest supersymmetric particle, is long-lived, and decays to a gravitino and either a Higgs or Z boson. This search is most sensitive to neutralino proper decay lengths of approximately 0.5 m, for which masses up to 1.18 TeV are excluded at 95% confidence level. The current search is the best result to date in the mass range from the kinematic limit imposed by the Higgs boson mass up to 1.8 TeV.

Keywords: Beyond Standard Model, Hadron-Hadron Scattering

ArXiv ePrint: 2212.06695

https://doi.org/10.1007/JHEP07(2023)210

JHEP07(2023)210

Contents

JHEP07(2023)210

1 Introduction

Many extensions of the standard model (SM) predict the existence of neutral, weakly coupled particles with long lifetimes. These long-lived particles (LLPs) naturally arise in supersymmetry (SUSY), e.g., in models with gauge-mediated SUSY breaking (GMSB) [1–3], split SUSY [4–9], SUSY with weak R-parity violation [10–13], and stealth SUSY [14, 15]. Other SM extensions also give rise to LLPs, including scenarios with hidden valleys [16–18], baryogenesis triggered by weakly interacting massive particles [19–21], inelastic dark matter [22], and twin Higgs mechanisms [23–25].

In this paper, we describe a search that focuses on LLPs that decay in the outer regions of the CMS tracker or within the calorimeters forming a signature with jets that are nearly trackless and out-of-time (delayed) with respect to the LHC collisions, hereafter

referred to as TD jets. This search uses a sample of proton-proton (pp) collisions collected in 2016–2018 at $\sqrt{s} = 13\,\text{TeV}$ with the CMS detector at the CERN LHC, corresponding to an integrated luminosity of $138\,\text{fb}^{-1}$. Jets produced by LLP decays that occur in the calorimeters or in the last few layers of the silicon tracker will have low track multiplicity compared to prompt jets that originate directly from the primary collision point. For simplicity, we will refer to such signal jets as trackless, though they may only be nearly so. Additionally, these signal jets will exhibit significant time delays with respect to those produced by SM backgrounds. The time delay arises from two different causes. The first cause, which dominates for LLP masses below about 400 GeV, is that LLP decays occur at macroscopic distances from the primary collision point, resulting in decay products that traverse a longer path to reach the calorimeters. The second cause, which dominates for LLP masses above about 600 GeV, is that high-mass LLPs travel measurably slower than the speed of light. The properties of the tracks and electromagnetic calorimeter (ECAL) hits associated with the jets are combined in a deep neural network (DNN) discriminator, which is used to distinguish between jets from LLP decays and those from SM backgrounds.

The ATLAS and CMS Collaborations have previously searched for LLPs using jets containing displaced tracks [26–30]. These searches rely on tracking information and thus yield excellent sensitivity to LLPs with proper decay lengths ($c\tau$), where τ is the lifetime of the LLP in its rest frame, below $\approx$0.2 m when the LLPs predominantly decay in the silicon trackers. Conversely, searches using displaced vertices in the ATLAS muon spectrometer [31] and a search by the CMS experiment using localized regions with high hit multiplicity in the muon system [32] result in excellent sensitivity to LLPs with $c\tau$ above 1 m. The search reported in this paper covers the intermediate $c\tau$ range, 0.3–1.0 m, and extends a previous CMS search using delayed jets [33] down to the kinematic limit imposed by the Higgs mass through the use of a dedicated TD jet tagger that makes optimal use of the time delay and trackless features of the jet.

While this search is sensitive to many models predicting LLPs, we interpret its results using a simplified model of GMSB chargino-neutralino production [34, 35]. The simplified model describes Higgsino-like charginos ($\widetilde{\chi}_1^{\pm}$) and neutralinos ($\widetilde{\chi}_1^0$, $\widetilde{\chi}_2^0$). All of them are assumed to be nearly degenerate in mass, with $\widetilde{\chi}_1^0$ being the lightest of them. They are produced in pairs in the following combinations: $\widetilde{\chi}_1^0\widetilde{\chi}_2^0$, $\widetilde{\chi}_1^0\widetilde{\chi}_1^{\pm}$, $\widetilde{\chi}_2^0\widetilde{\chi}_1^{\pm}$, and $\widetilde{\chi}_1^{\pm}\widetilde{\chi}_1^{\mp}$. Because of the near mass-degeneracy, both $\widetilde{\chi}_2^0$ and $\widetilde{\chi}_1^{\pm}$ decay to $\widetilde{\chi}_1^0$ and to other low transverse momentum (p_T) particles, leading to effective $\widetilde{\chi}_1^0$ pair production. Each $\widetilde{\chi}_1^0$ will subsequently decay to a Higgs or Z boson and a gravitino ($\widetilde{\text{G}}$), which is the lightest SUSY particle, thus conserving R-parity. The search focuses on hadronic decays of the Higgs or Z boson. Signal events typically have large missing transverse momentum resulting from the momentum of the gravitinos, which do not interact with the detector, or from the Lorentz boost of the neutralino when the neutralino decays outside of the calorimeter volume. Feynman diagrams of the effective neutralino pair production in the simplified model are shown in figure 1.

The rest of this paper is organized as follows. A brief description of the CMS detector is given in section 2. Section 3 provides a summary of the various simulated samples used in the analysis. The event reconstruction and selection are described in section 4, while the DNN-based TD jet discriminator is discussed in section 5. The background estimation and systematic uncertainties are detailed in sections 6 and 7, respectively. We report and

JHEP07(2023)210

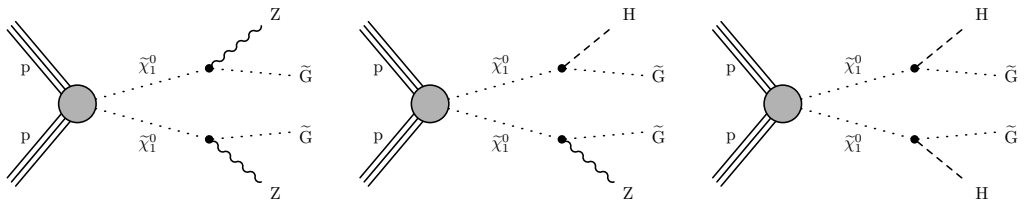

Figure 1. Feynman diagrams of the effective neutralino pair production in the GMSB simplified model in which the two neutralinos decay into two gravitinos ($\widetilde{G}$) and two Z bosons (left), a Z and a Higgs boson (H) (center), or two Higgs bosons (right).

interpret the results in section 8. Finally, a summary is given in section 9. The detailed results of this paper are found in the associated HEPData record [36].

2 The CMS detector

The central feature of the CMS detector is a superconducting solenoid of 6 m internal diameter, providing a magnetic field of 3.8 T. Within the solenoid volume are a silicon pixel and strip tracker, a lead tungstate crystal ECAL, and a brass and scintillator hadron calorimeter (HCAL), each composed of a barrel and two endcap sections.

The ECAL consists of 75 848 lead tungstate crystals, which cover $|\eta| < 1.48$ in the barrel region and $1.48 < |\eta| < 3.00$ in the two endcap regions. The excellent signal-to-noise ratio and stable pulse shape of the ECAL sensors allow for timing measurements with the best resolution achievable at very large energies of better than 100 ps per hit [37]. The HCAL is composed of cells of width 0.087 in η and azimuth (ϕ, in radians) for the region $|\eta| < 1.74$, progressively increasing to a maximum of 0.174 for larger values of $|\eta|$, along with the forward calorimeters extending the η coverage provided by the barrel and endcap detectors. The outer tracker layers extend to a radial distance of 1.16 m in the barrel; the front face of the ECAL crystals are located at a radial distance of 1.29 m, and the crystals extend radially for 23 cm; and the HCAL covers the radial distances between 1.77 and 2.95 m. Muons are measured in the range $|\eta| < 2.4$, with detection planes embedded in the steel flux-return yoke outside the solenoid and made using three technologies: drift tubes (DTs), cathode strip chambers (CSCs), and resistive-plate chambers.

Events of interest are selected using a two-tiered trigger system. The first level, composed of custom hardware processors, uses information from the calorimeters and muon detectors to select events at a rate of around 100 kHz within a fixed latency of about 4 μs [38]. The second level, known as the high-level trigger, consists of a farm of processors running a version of the full event reconstruction software optimized for fast processing, and reduces the event rate to around 1 kHz before data storage [39]. A more detailed description of the CMS detector, together with a definition of the coordinate system used and the relevant kinematic variables, can be found in ref. [40].

JHEP07(2023)210

3 Simulated samples

Several simulated event samples are used to model the signal and SM background processes, and as training samples for the TD jet discriminator. Samples of top quark-antiquark pair ($\mathrm{t\bar{t}}$) and single top quark events, W+jets and Z+jets (collectively called V+jets) events, and events composed uniquely of jets produced through the strong interaction, referred to as quantum chromodynamics (QCD) multijet events, are produced with the Monte Carlo (MC) generator MadGraph5_aMC@NLO 2.2.2 [41] at leading-order (LO). Up to three and four additional partons are considered in the matrix element (ME) calculations for the generation of the V+jets and top quark samples, respectively. The MLM jet matching scheme [42, 43] is used. The background samples are normalized according to the most precise cross section calculations available, typically corresponding to next-to-LO (NLO) or next-to-NLO (NNLO) precision [41, 44–47].

The SUSY signal samples are generated at LO in perturbative QCD using the MadGraph5_aMC@NLO 2.4.2 generator [41] with up to two additional partons in the final state at the ME level, and using the MLM jet matching scheme. The corresponding cross sections for effective $\widetilde{\chi}_1^0\widetilde{\chi}_1^0$ production, assuming nearly mass-degenerate Higgsino-like $\widetilde{\chi}_1^\pm$, $\widetilde{\chi}_2^0$, and $\widetilde{\chi}_1^0$, are computed to NLO precision including next-to-leading logarithmic corrections [48–55]. In the calculation, all SUSY particles other than $\widetilde{\chi}_1^\pm$, $\widetilde{\chi}_2^0$, $\widetilde{\chi}_1^0$, and $\widetilde{\mathrm{G}}$ are assumed to be too heavy to participate in the interaction. We follow the convention of real mixing matrices and signed masses for the neutralinos and charginos [56] used in previous CMS searches [57, 58].

For the simulated samples corresponding to the 2016 data-taking period, the NNPDF v3.0 LO and NLO parton distribution functions (PDFs) [59, 60] are used for samples generated at LO and NLO, respectively. For the simulated samples corresponding to the 2017–2018 data-taking periods, the NNPDF v3.1 NNLO PDFs are used. The simulated events at the ME level are interfaced with pythia 8.226 [61] or a later version to simulate the shower and hadronization of partons, and the underlying event description. The CUETP8M1 [62] and CP5 [63] tunes are used for the simulated samples corresponding to the 2016 and 2017–2018 data-taking periods, respectively.

For all simulated samples, the detector response is modeled using a detailed description of the CMS detector based on Geant4 [64]. Object and event reconstruction are performed with the same algorithms as are used for the CMS data. Minimum bias events are superimposed on each simulated hard scattering event to reproduce the effect of extra pp interactions within the same or neighboring bunch crossings as the recorded event (pileup). Events are weighted such that the distribution of the number of interactions per bunch crossing agrees with that observed during each data-taking period.

4 Event reconstruction and selection

The particle-flow (PF) algorithm [65] aims to reconstruct and identify each individual particle in an event as an electron, photon, muon, charged or neutral hadron, with an optimized combination of information from the various elements of the CMS detector.

JHEP07(2023)210

These reconstructed particles are referred to as PF candidates. Photons are identified as ECAL energy clusters not linked to the extrapolation of any charged particle trajectory to the ECAL [66]. The energy of photons is obtained from the ECAL measurement. Electrons are identified as a primary charged particle track and potentially many ECAL energy clusters corresponding to this track extrapolation to the ECAL and to possible bremsstrahlung photons emitted along the way through the tracker material [67, 68]. The electron momentum is estimated by combining the energy measurement in the ECAL with the momentum measurement in the tracker. Muons are identified as tracks in the central tracker consistent with either a track or several hits in the muon system, and associated with calorimeter deposits compatible with the muon hypothesis. Hadronically decaying τ leptons are reconstructed with the hadron-plus-strips (HPS) algorithm [69, 70] on the basis of the number of tracks and of the number of ECAL strips in the η-ϕ plane with energy deposits, in the 1-prong, 1-prong + π^0, and 3-prong decay modes. A cut-based selection based on isolation sums [70] is used to suppress the rate for quark- and gluon-initiated jets to be misidentified as hadronic τ candidates.

Charged hadrons are identified as charged particle tracks neither identified as electrons, nor as muons. The energy of charged hadrons is determined from a combination of the track momentum and the corresponding ECAL and HCAL energies, corrected for the response function of the calorimeters to hadronic showers. Finally, neutral hadrons are identified as HCAL energy clusters not linked to any charged hadron trajectory, or as a combined ECAL and HCAL energy excess with respect to the expected charged hadron energy deposit. The energy of neutral hadrons is obtained from the corresponding corrected ECAL and HCAL energies.

For each event, hadronic jets are clustered from PF candidates using the infrared- and collinear-safe anti-k_T algorithm [71, 72] with a distance parameter of 0.4. The jet momentum is determined as the vector sum of all particle momenta in the jet, and is found from simulation to be, on average, within 5–10% of the true momentum over the entire p_T spectrum and detector acceptance. Although charged particles resulting from LLP decays that occur farther from the interaction point may be misidentified as neutral PF candidates, their contribution to the jet energy scale and resolution is correctly accounted for on average. Pileup interactions can produce additional tracks and calorimetric energy depositions, increasing the apparent jet momentum. To mitigate this effect, tracks consistent with pileup vertices are discarded and an offset correction is applied to correct for remaining contributions. We have verified that this pileup mitigation procedure does not reduce the signal efficiency. Jet energy corrections are derived from simulation studies so that the average measured energy of jets becomes identical to that of particle level jets. In situ measurements of the momentum balance in dijet, photon+jet, Z+jet, and multijet events are used to determine any residual differences between the jet energy scale in data and in simulation, and appropriate corrections are made [73]. Using Z+jet events, we verified that these jet energy corrections, as well as their uncertainties, remain accurate when applied to jets with high scores of the TD jet tagger. The jet energy resolution amounts typically to 15–20% at 30 GeV, 10% at 100 GeV, and 5% at 1 TeV [73].

JHEP07(2023)210

The vector $\vec{p}_{\mathrm{T}}^{\,\mathrm{miss}}$ is computed as the negative vector p_{T} sum of all the PF candidates in an event, and its magnitude is denoted as $p_{\mathrm{T}}^{\mathrm{miss}}$ [74]. The primary vertex (PV) is taken to be the vertex corresponding to the hardest scattering in the event, evaluated using tracking information alone, as described in section 9.4.1 of ref. [75].

4.1 Jet time reconstruction

Jets from signal events arrive at the ECAL later than particles produced at the PV by 1–10 ns, depending on the LLP mass. Therefore, measuring the jet time delay with respect to a particle produced at the PV and traveling at the speed of light helps to discriminate between signal and background. The time of arrival of a jet at the ECAL, t_{ECAL}, is calculated based on an energy-weighted sum of the arrival times reconstructed from the signal pulses in each ECAL crystal associated with the jet

$$t_{\mathrm{ECAL}} = \frac{\sum_{i=1}^{N_{\mathrm{crystal}}} t_{\mathrm{ECAL}}^{i} E_{\mathrm{ECAL}}^{i}}{\sum_{i=1}^{N_{\mathrm{crystal}}} E_{\mathrm{ECAL}}^{i}}, \tag{4.1}$$

where t_{ECAL}^{i} and E_{ECAL}^{i} are the timestamp and reconstructed energy of the signal pulse in crystal i, respectively, and N_{crystal} is the number of crystals associated with the jet. Details of the ECAL time reconstruction algorithm and performance can be found in ref. [76]. Accounting for clock jitter, collision beam spot size, and time-dependent calibration effects, the effective jet time resolution is $\sim$ 400–600 ps for jets with p_{T} ranging from 30–150 GeV. During collisions, there are variations in the clock signal distribution between different regions of the ECAL and different LHC fills, which are corrected using special calibration data, but these corrections may be imperfect. As a result, there may be a degradation in the time resolution for jets [77]. We validate and correct, where necessary, the simulated prediction of the jet time mean and resolution using a pure sample of b-tagged jets from dilepton $\mathrm{t\bar{t}}$ events. The high purity of the b-tagged jets from the dilepton $\mathrm{t\bar{t}}$ sample ensures that the jet time measurement is not contaminated by pileup jets, which have a different timing response. We apply a Gaussian smearing procedure [73]: the jet time in the $\mathrm{t\bar{t}}$ simulation sample is multiplied by a random number drawn from a Gaussian distribution. We determine the Gaussian mean and standard deviation parameters that minimize the χ^2 test statistic [78] calculated between the data and the simulation-based prediction. The same jet time correction is also applied to the signal simulation, and the correction uncertainties are propagated to the TD jet tagger efficiency. The systematic uncertainties in the signal yield resulting from the time correction range from 3 to 18%, generally increasing with decreasing $\widetilde{\chi}_1^0$ mass.

4.2 Event selection

Events for this search are collected with a trigger requiring $p_{\mathrm{T}}^{\mathrm{miss}} > 120$ GeV [39] when reconstructed online. We define a preselection by requiring events to have $p_{\mathrm{T}}^{\mathrm{miss}} > 200$ GeV when reconstructed offline, which ensures a trigger selection efficiency above 99%. Background events can occur because of mismeasurement of high-p_{T} jets, which results in the alignment of the ϕ coordinates of $\vec{p}_{\mathrm{T}}^{\,\mathrm{miss}}$ and the nearby mismeasured jet. The $\Delta\phi_{\mathrm{min}}$ is

JHEP07(2023)210

defined as the ϕ angle between $\vec{p}_{\mathrm{T}}^{\,\mathrm{miss}}$ and the closest jet with $p_{\mathrm{T}} > 30\,\mathrm{GeV}$. For the QCD multijet background, the $\Delta\phi_{\mathrm{min}}$ distribution is predominantly near zero, while for signal events the distribution is more uniform because the $p_{\mathrm{T}}^{\mathrm{miss}}$ results from the $\widetilde{\mathrm{G}}$ escaping the detector rather than any of the jets being mismeasured. We select events with $\Delta\phi_{\mathrm{min}} > 0.5$, reducing the QCD multijet background by one order of magnitude while retaining 70–85% of the signal events.

The main tool used in this analysis to differentiate between signal and background is the TD jet tagger, discussed in section 5. We consider jets with $p_{\mathrm{T}} > 30\,\mathrm{GeV}$ and $|\eta| < 1.0$, and count the number of jets that pass the TD jet tagger selection defined in section 5. Jets in the barrel region of the detector with $|\eta|$ between 1.00–1.48 are not considered because the rate of background jets passing the TD jet tagger selection is significantly larger due to higher tracking inefficiency in this region. To ensure that jets primarily composed of nonisolated muons, electrons, or photons are not misidentified as TD-tagged jets, we veto any jet with the energy fractions of these particles larger than 0.6, 0.6, or 0.8, respectively. In addition, jets that are within $\Delta R = \sqrt{(\Delta\phi)^2 + (\Delta\eta)^2} = 0.4$ of any identified and isolated muon, electron, or photon are also not considered.

To suppress background from W+jets and $\mathrm{t\bar{t}}$, we reject any event with an identified and isolated muon, electron, or hadronically decaying tau candidate. The number of TD-tagged jets (N_{TDJ}) is used to define the different data samples used in the analysis. The signal region (SR) is defined as one comprising events with $N_{\mathrm{TDJ}} \geq 2$. To estimate the background in the SR, a background-enriched control region (CR) that comprises events with exactly one TD-tagged jet is used. Events with zero TD-tagged jets are also expected to arise primarily from background processes and are used to validate the background estimation method, as described in section 6. Because of the large background suppression factor exceeding 10^3 from the presence of each additional TD-tagged jet, the impact of signal contamination in the zero and one TD-tagged jet region on the analysis sensitivity was found to be less than 1%.

4.3 Cosmic ray muon and beam halo vetoes

Noncollision backgrounds from cosmic ray muons or beam halo particles are typically trackless because their trajectories do not coincide with the luminous region known as the beam spot, which the track reconstruction algorithm assumes to be the origin of particle trajectories [79]. Because we require at least two TD-tagged jets, these noncollision backgrounds only enter the SR if the particles are oriented in specific ways. Given the specific trajectory configurations required, such backgrounds are rare. To suppress them to negligible levels, we use particular features of such events to veto them.

Collisions between beam protons and an upstream collimator can result in beam halo particles that pass through the calorimeter volume parallel to the beam axis. These beam halo particles may induce localized energy deposits in the calorimeters causing delayed signals that are misreconstructed as multiple jets with nearly equal ϕ coordinates [74]. In addition, such jets tend to have a very small number of ECAL hits. Therefore, we veto events in which the two TD-tagged jets have $|\Delta\phi| < 0.05$ and at least one of the two jets has 10 or fewer ECAL hits. This veto has a signal efficiency between 98 and 100% depending on

JHEP07(2023)210

the signal mass and $c\tau$. Events are also rejected by the so-called CSC beam halo filter [74] if they contain reconstructed tracks parallel to the beam axis using segments in the CSCs.

Events containing a cosmic ray muon can enter the SR if the muon traverses the calorimeter volume without passing through the tracker, producing localized energy deposits that can give rise to multiple apparent jets that are delayed in time. Cosmic ray muon background events can be identified by the presence of track segments in the DT muon detector planes, which lie on a line with the calorimeter hits comprising the jets. Segments are clustered with a density-based algorithm [80] and a minimum distance parameter of 1.4 m, and segments from at least three different sets of DT muon detector planes are required in each cluster. If two or more DT segment clusters are found, the geometric centroid positions of the two clusters closest to the calorimeter hits of the jets in the z coordinate are used to define a line. If the distance of closest approach from the centroid of the ECAL hits to the line is less than 0.5 m, then the event is interpreted as a cosmic ray muon event and rejected from the SR and CRs. This veto has a signal efficiency larger than 99.9%.

5 Trackless delayed jet tagger

Jets produced by LLPs that decay in the outer region of the CMS tracking volume or inside the calorimeters tend to be trackless and delayed in time, features that are not exhibited by SM backgrounds. We trained a DNN to optimally exploit these features for discriminating between TD and SM jets.

The TD jet tagger is based on information from tracks, PF candidates, and calorimeter hits associated with the jet, expressed as 22 input features. The tracking-related observables we use include the number of and scalar p_{T} sum of tracks in the jet, the scalar p_{T} sum of tracks matched to the PV in the jet, the minimum ΔR values between the jet axis and any track as well as between the jet axis and any track associated with the PV, and three variables sensitive to pileup: α_{max}, β_{max}, and γ_{max}. These variables are defined as

$$\alpha_{\mathrm{max}} = \frac{\max_{\mathrm{trk}\in\mathrm{jet}\cap\mathrm{PV}} p_{\mathrm{T}}^{\mathrm{trk}}}{\sum_{\mathrm{trk}\in\mathrm{jet}} p_{\mathrm{T}}^{\mathrm{trk}}}, \beta_{\mathrm{max}} = \frac{\max_{\mathrm{trk}\in\mathrm{jet}\cap\mathrm{PV}} p_{\mathrm{T}}^{\mathrm{trk}}}{p_{\mathrm{T}}^{\mathrm{jet}}}, \gamma_{\mathrm{max}} = \frac{\max_{\mathrm{trk}\in\mathrm{jet}\cap\mathrm{PV}} p_{\mathrm{T}}^{\mathrm{trk}}}{E^{\mathrm{jet}}}, \quad (5.1)$$

where $\mathrm{trk} \in \mathrm{jet} \cap \mathrm{PV}$ denotes the track that belongs to the jet and is associated with the PV, $\mathrm{trk} \in \mathrm{jet}$ denotes the track that belongs to the jet, $p_{\mathrm{T}}^{\mathrm{trk}}$ is the track p_{T}, and $p_{\mathrm{T}}^{\mathrm{jet}}$ and E^{jet} are the jet p_{T} and energy, respectively. The energy fractions associated with hadrons, electrons, and photons, and the number of PF candidate constituents of the jet are also used as inputs to the TD jet tagger. Finally, several variables calculated using ECAL hits associated with the jet are used: the number of ECAL hits in the jet, the ratio of the energy sum of all ECAL hits in the jet to E^{jet}, the jet time calculated as in eq. (4.1), the semi-major and semi-minor axes of the ECAL hits in the jet [37], and the fragmentation function. The latter is a function that describes how the ECAL hits contribute to the jet energy considering their multiplicity [81]. Jets from signal LLP decays tend to have low values of α_{max}, β_{max}, γ_{max}, charged energy fraction, semi-major and semi-minor axes, and the fragmentation function, and large values of ΔR between the jet axis and tracks. The charged and neutral energy fractions are lower and higher, respectively, for signal jets than

JHEP07(2023)210

for background jets not because the jet composition is different, but rather because the PF algorithm misidentifies the particle types because of reduced tracking efficiency for charged particles produced at large displacement.

Simulation samples are used to train and evaluate the performance of the DNN. The signal sample consists of GMSB signal events with a $\widetilde{\chi}_1^0$ mass of 400 GeV and $c\tau$ of 1 m. These events are used only for training or evaluating the performance of the DNN and are not used to predict the signal yields for the final statistical analysis. This $\widetilde{\chi}_1^0$ mass was chosen for the training sample because our search targets the low-mass range starting from the kinematic limit imposed by the Higgs boson mass, where previous searches have limited sensitivity. In signal events, the Higgs or Z boson, produced by the decay of the LLP, subsequently decays to a pair of partons that can each be reconstructed as a displaced jet. Such jets are labeled as signal jets if they geometrically coincide with a parton that originates from LLP decays that occur between the last layers of the tracker and the outer surface of the HCAL (decay radii between 0.30 and 1.84 m). Jets are required to have $|\eta| < 1.48$ to be included in the training sample. This selection is further restricted to $|\eta| < 1$ in the search to improve the final signal-to-background ratio as the background increases in the higher η range because of tracking inefficiencies. Background samples consist of a mixture of QCD multijet, W+jets, $\mathrm{Z}(\nu\overline{\nu})$+jets, and $\mathrm{t\overline{t}}$ events weighted in proportion to their production cross sections. The signal and background samples obtained after applying the selections described in section 4.2 contain 0.3 and 2.2 million events, respectively. The samples are split into training, validation, and testing sets, accounting for 40, 10, and 50% of the full set, respectively. The validation set is used to evaluate the training process and monitor for overfitting, while the testing set is used to measure the final performance after training. We show comparisons between the simulation prediction and the observed data distributions for a few key input variables to the TD jet tagger in appendix A, confirming that the simulation provides an accurate description.

A fully connected DNN architecture was developed with machine learning software frameworks Keras [82] and TensorFlow [83]. The network architecture consists of four fully connected hidden layers, with 64, 32, 16, and 8 nodes, respectively, and an output layer with two nodes, corresponding to the two classes, signal and SM background. Rectified linear unit [84, 85] activation functions are used in the hidden layers, while a softmax activation function [86, 87] is applied to the output layer, and a 10% dropout rate [88] is applied to all layers to prevent overfitting. We use a batch size of 512, categorical cross entropy as the loss function, and the Adam optimizer [89] with an initial learning rate of 10^{-3}. Training is performed for up to 1 000 epochs, or cycles, over the full training set. Early stopping is applied to mitigate overfitting: after each epoch, the loss function is evaluated on the validation set and the training process is interrupted if after 100 successive epochs, the validation loss has not decreased. The model corresponding to the smallest validation loss is used.

The most impactful input variables are the charged and neutral hadron energy fractions, the number of track constituents in the jet, the ΔR between the jet axis and the closest track associated with the PV, and the jet time. Their distributions for signal and collision background events are shown in figure 2. Noncollision backgrounds are not included. The distribution of the TD jet tagger score for the testing set is shown in figure 3

JHEP07(2023)210

(left), demonstrating the excellent discrimination of the tagger. The identification probability for the signal versus the misidentification probability for the background is shown in figure 3 (right). In the search, jets are tagged as signal if the TD jet tagger score is larger than 0.996, chosen to yield the best signal sensitivity. The signal efficiency of the TD jet tagger is shown in figure 4 as a function of the transverse decay length in the lab frame, and on average the background efficiency is about 4×10^{-4} per candidate jet.

5.1 Signal efficiency modeling

The input features of the TD jet tagger making the largest contributions to the signal-to-background discrimination are those related to the trackless nature of signal jets. For these features, the simulation has not yet been extensively validated. To perform this validation and measure the accuracy of the simulation for the TD jet tagger signal efficiency, we use either photons or electrons as proxy objects to represent the LLP decays that occur in the outer tracking or calorimeter volume. Photons, or electrons with their own tracks removed from consideration, are the best approximations to trackless jets that we can effectively isolate in collision events.

Having corrected and validated the simulation of the jet time response as described in section 4.1, we proceed to validate the accuracy of the simulation prediction of the TD tagger discriminator, after factorizing the impact of the jet time measurement. This is achieved by replicating the time of arrival distribution for signal jets in the corresponding distribution for prompt proxy objects through the introduction of an artificial delay of 1–2 ns, which is sufficient to cover the bulk of the expected TD tagger scores for signal jets. Whether to use photons or electrons is based on the jet p_{T}. A sample of photons is obtained by selecting $\mathrm{Z} \to \ell^{+}\ell^{-}\gamma$ events in which one of the leptons (ℓ = muon or electron) radiates a photon. We require the mass of the $\ell^{+}\ell^{-}\gamma$ system to be between 70–110 GeV to ensure that the sample is not contaminated by jets misidentified as photons. Because the photon in the $\mathrm{Z} \to \ell^{+}\ell^{-}\gamma$ sample has a relatively soft momentum spectrum, this control region is only valid for LLP candidate jets with $p_{\mathrm{T}} < 70$ GeV.

For LLP candidate jets with $p_{\mathrm{T}} > 70$ GeV, we use electrons from $\mathrm{W} \to \mathrm{e}\nu_{\mathrm{e}}$ events as proxy objects obtained by selecting events with an electron passing standard isolation and identification criteria [67] and $p_{\mathrm{T}}^{\mathrm{miss}} > 70$ GeV. The distributions of the TD jet tagger input variables for the photons and electrons in data and simulation are smeared to match the distributions for displaced jets from signal events. To calculate all the tagger input variables, the track produced by the electron candidate is removed, and the electron is treated as a photon. We evaluate the TD jet tagger scores for these proxy objects after the corrections to the input variables and imposing the artificial time delay, shown in figure 5, and measure the efficiency for such proxy objects to have a TD jet tagger score larger than 0.996, the threshold used to tag signal jets. The measured efficiencies are compared to the efficiencies predicted by the simulation, and data-to-simulation correction factors are obtained; these factors show no dependence on jet p_{T} and η, and are all in the range 0.9–1.1. The difference in the correction factor obtained from imposing a delay of 1 and 2 ns is propagated as a systematic uncertainty.

JHEP07(2023)210

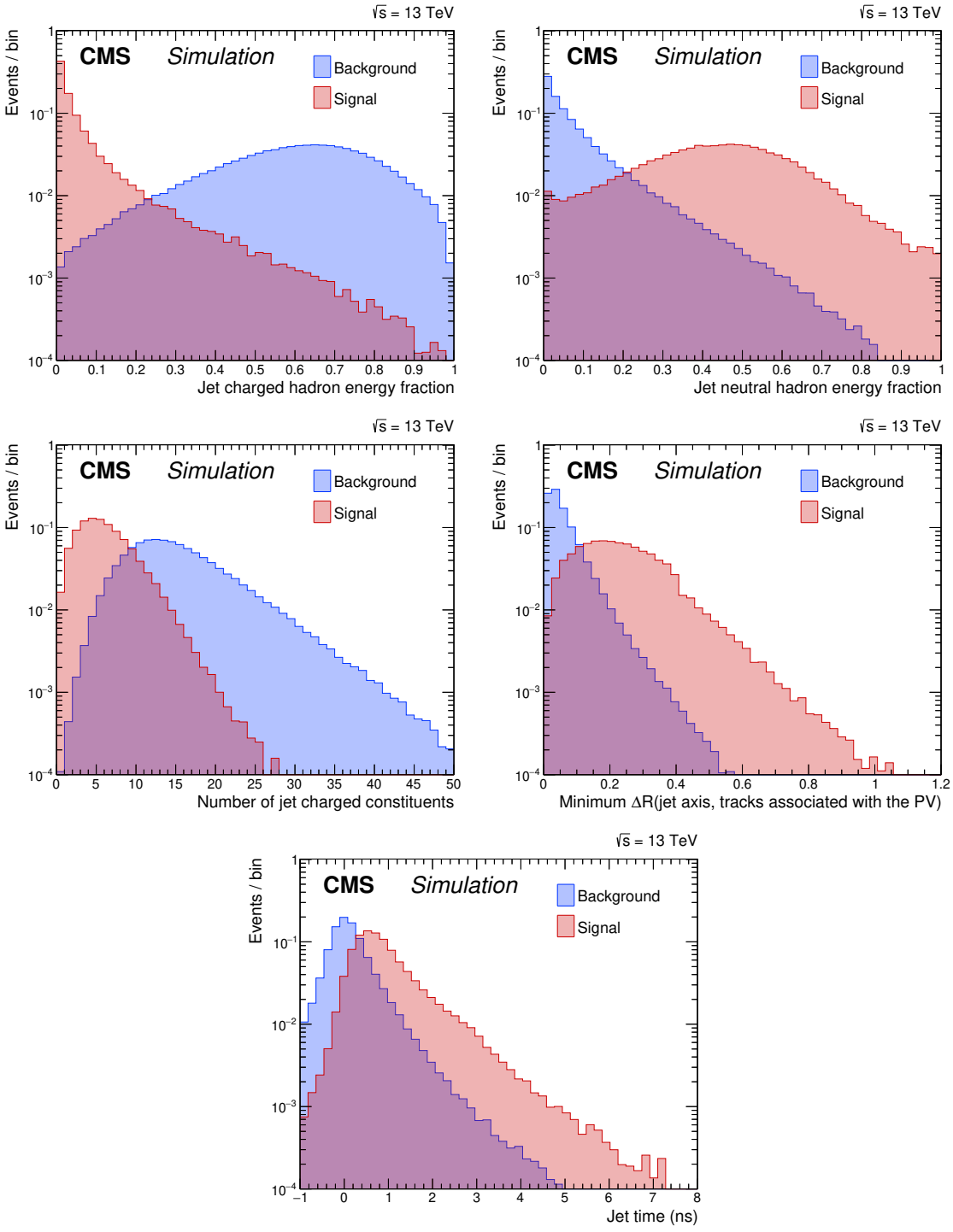

Figure 2. The distributions of the most impactful input variables to the TD jet tagger for signal (red, lighter) and collision background (blue, darker). They include the charged (upper left) and neutral (upper right) hadron energy fractions, the number of track constituents in the jet (middle left), the minimum ΔR between the jet axis and the closest track associated with the PV (middle right), and the jet time (lower).

JHEP07(2023)210

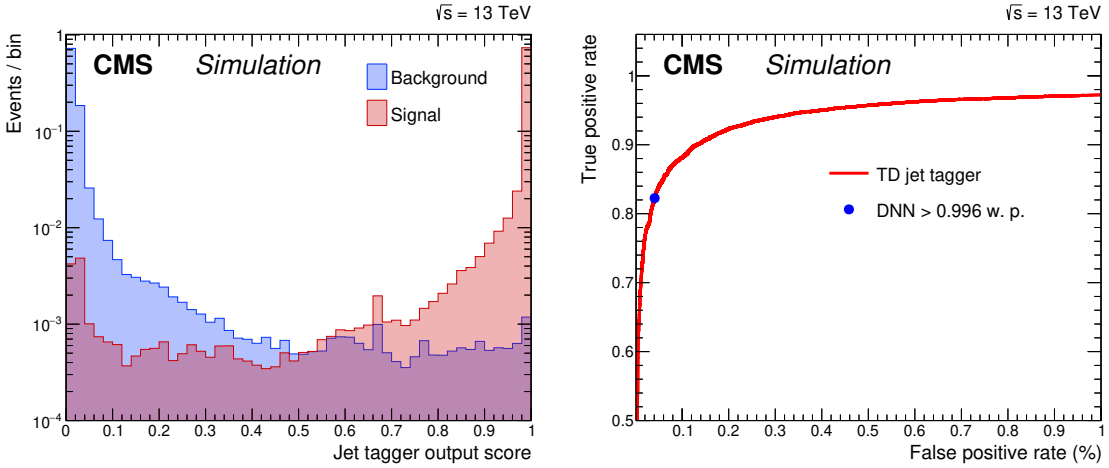

Figure 3. TD jet tagger score distributions (left) for signal (red, lighter) and collision background (blue, darker). Identification probability for the signal versus the misidentification probability for the background (right) with the tagger working point (w. p.) used in the analysis shown as a blue marker. Both are evaluated using an independent sample of testing events.

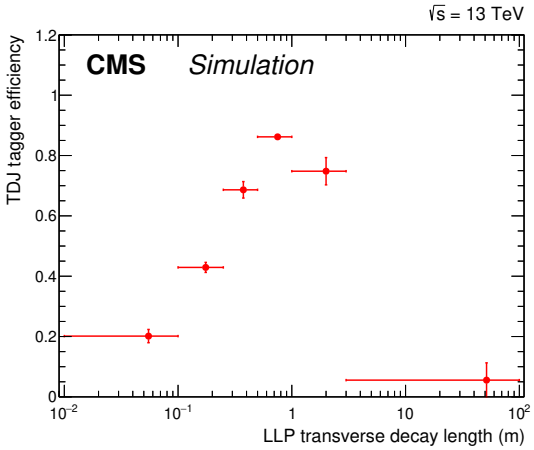

Figure 4. The efficiency of the TD jet tagger working point used in the analysis is shown as a function of the lab frame transverse decay length for simulated signals with $\widetilde{\chi}_1^0$ mass of 400 GeV. The uncertainties shown account for lifetime dependence and statistical uncertainty.

6 Background estimation

The main background processes are QCD multijet, W+jets, Z($\nu\bar{\nu}$)+jets, and $t\bar{t}$ production, where prompt jets have been misidentified as signal jets by the TD jet tagger. The misidentification occurs very rarely, less than 0.1% as shown in figure 6, and results primarily from outliers in the jet composition and in the time measurement. The prompt jets that pass the TD jet tagger either result from tracking inefficiencies or from instances where the fragmentation and hadronization is mostly into photons or neutral hadrons, rendering such jets approximately trackless. Misidentified jets can also have larger measured times,

JHEP07(2023)210

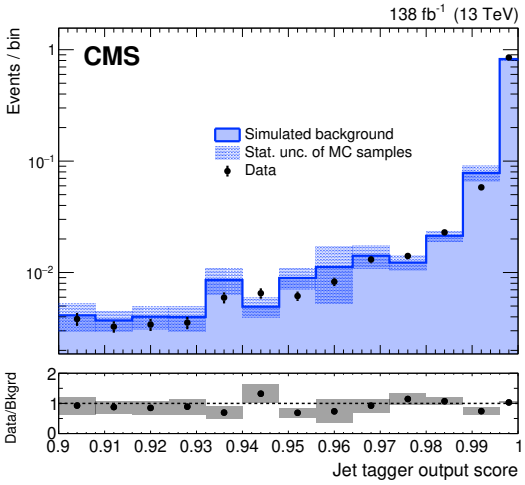

Figure 5. The TD jet tagger score distributions for simulation (shaded histogram) and data (black markers) when using electrons from $\mathrm{W} \to \mathrm{e}\nu_\mathrm{e}$ events as proxy objects for signal jets. The histograms and data points have been normalized to unit area. The last bin contains jets with tagger scores greater than 0.996, the threshold used to tag signal jets. Similar levels of agreement are observed for photon proxy objects from the $\mathrm{Z} \to \ell^+\ell^-\gamma$ sample.

making them appear to be delayed. Because the misidentification primarily results from instrumental and resolution effects, the misidentification probability per jet ϵ_bkg does not depend strongly on the process or the presence of other objects in the event. Motivated by these observations, we employ a matrix method [90, 91] to estimate the background contribution to the two-tag SR.

Jets with $p_\mathrm{T} > 30\,\mathrm{GeV}$ are defined as the basic objects used for the matrix method. We measure ϵ_bkg in signal-depleted measurement regions (MRs) as a function of jet η. It is sufficient to parameterize ϵ_bkg only as a function of jet η because we observe that it is independent of the jet p_T. The nominal MR is obtained by selecting events with one electron or muon with $p_\mathrm{T} > 35$ or $30\,\mathrm{GeV}$, respectively, passing standard isolation and identification criteria [67, 92]. The events are also required to have $p_\mathrm{T}^\mathrm{miss} > 40\,\mathrm{GeV}$ to suppress QCD multijet background, and to have transverse mass smaller than $100\,\mathrm{GeV}$ to suppress a potential beyond the SM signal. The ϵ_bkg measurement, derived per jet, is shown in figure 6, for two data-taking years. The misidentification probability is significantly greater for the first $19.9\,\mathrm{fb}^{-1}$ of data collected in 2016 because of the impact of suboptimal settings on the tracker readout chip in the presence of large pileup. The readout chip parameters were reoptimized for the later part of 2016, resulting in improved tracking efficiency and less misidentification for the last $16.4\,\mathrm{fb}^{-1}$ of data collected in 2016.

To quantify the degree of process dependence, misidentification probabilities from three alternative MRs are measured. The Z+jets MR, intended to represent the $\mathrm{Z}(\nu\overline{\nu})$+jets background, is obtained by selecting events with two electrons or two muons, each satisfying the $p_\mathrm{T} > 35$ or $30\,\mathrm{GeV}$ requirement, respectively, and requiring the dilepton mass to be between 60 and 120 GeV. The $p_\mathrm{T}^\mathrm{miss}$ is required to be less than $30\,\mathrm{GeV}$ to suppress other background processes. Likewise, the $\mathrm{t\bar{t}}$ MR is obtained by selecting events with one electron

JHEP07(2023)210

Measurement region	Selection
Nominal	1 electron (muon) with $p_{\mathrm{T}} > 35$ (30) GeV, $p_{\mathrm{T}}^{\mathrm{miss}} > 40$ GeV, $m_{\mathrm{T}} < 100$ GeV
Z+jets	2 electrons (2 muons) with $p_{\mathrm{T}} > 35$ (30) GeV, $60 < m_{\mathrm{ee}}$ ($m_{\mu\mu}$) < 120 GeV, $p_{\mathrm{T}}^{\mathrm{miss}} < 30$ GeV
$\mathrm{t\bar{t}}$	1 electron and 1 muon with $p_{\mathrm{T}} > 35$ and 30 GeV, $p_{\mathrm{T}}^{\mathrm{miss}} > 30$ GeV
QCD multijet	1 jet with $p_{\mathrm{T}} > 140$ GeV online, $p_{\mathrm{T}}^{\mathrm{miss}} < 25$ GeV offline

Table 1. Definitions of the measurement regions used to quantify the process dependence of the TD jet misidentification probability.

and one muon, with the same p_{T} requirements described above, and $p_{\mathrm{T}}^{\mathrm{miss}} > 30$ GeV. Events in the QCD multijet MR are required to have a jet with $p_{\mathrm{T}} > 140$ GeV online, and $p_{\mathrm{T}}^{\mathrm{miss}} < 25$ GeV offline to avoid signal contamination. A summary of the different MRs can be found in table 1. The envelope covering the range of misidentification probabilities measured in the nominal and three alternative MRs is used to derive a systematic uncertainty. This systematic uncertainty quantifying the degree of process dependence is shown in figure 6 and found to be 45% relative to the collision background and 30% relative to the total background prediction.

To predict the number of background events in the two-tag SR, we consider each untagged jet i with $p_{\mathrm{T}} > 30$ GeV in events passing the preselection with exactly one TD-tagged jet and assign it a probability $\epsilon_{\mathrm{bkg}}(\eta_{\mathrm{jet}\ i})$ to be misidentified as a TD jet. Each untagged jet in the event is treated independently, and the total background prediction $N_{\geq 2\text{-tag bkg}}$ is obtained from the sum

$$N_{\geq 2\text{-tag bkg}} = \sum_{k=1}^{N_{1\text{-tag}}} \left(\sum_{i=1}^{N_{\mathrm{untagged}}^{k}} \epsilon_{\mathrm{bkg}}(\eta_{\mathrm{jet}\ i}) \right), \tag{6.1}$$

where $N_{1\text{-tag}}$ is the number of one-tag events in data and $N_{\mathrm{untagged}}^{k}$ is the number of untagged jets in event k. This prediction ignores contributions of order $\epsilon_{\mathrm{bkg}}^{2}$ and is accurate in the limit where ϵ_{bkg} is very small, which is the case here as ϵ_{bkg} is below 10^{-3}. Using the matrix method described above, we predict a collision background yield of 0.15 ± 0.08 (stat + syst) for the two-tag SR.

An alternative background prediction $N'_{\geq 2\text{-tag bkg}}$ is obtained by selecting events with zero TD-tagged jets and considering each pair of untagged jets (jets i and j) as a potential source of misidentified jets. Each untagged jet pair is assigned a weight

JHEP07(2023)210

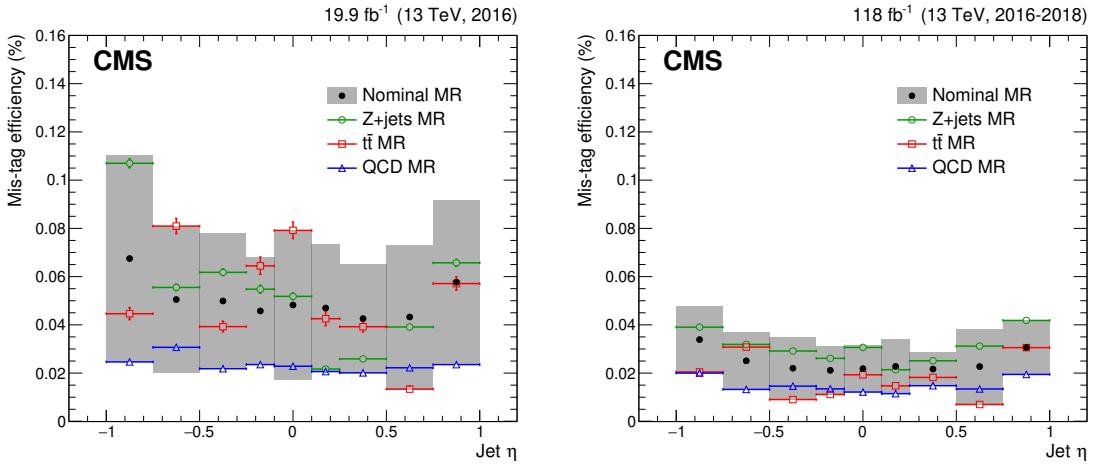

Figure 6. The TD jet tagger misidentification probability measured using the nominal W+jets MR (black round markers) is shown along with the systematic uncertainty (gray band), quantifying the degree of process dependence measured from alternative MRs. The measurements in the alternative MRs are displayed as well (Z+jets MR as green round markers, $t\bar{t}$ MR as red squared markers, QCD MR as blue triangular markers) along with their respective statistical uncertainty. On the left, this probability is shown for the first 19.9 fb^{-1} of data collected in 2016, while on the right it is shown for the last 16.4 fb^{-1} of data collected in 2016 combined with data collected in 2017–2018.

$\epsilon_{\text{bkg}}(\eta_{\text{jet }i})\epsilon_{\text{bkg}}(\eta_{\text{jet }j})$, and the alternative background prediction is given by

$$N'_{\geq 2\text{-tag bkg}} = \sum_{k=1}^{N_{0\text{-tag}}} \left(\sum_{i=1}^{N^k_{\text{untagged}}} \sum_{j>i}^{N^k_{\text{untagged}}} \epsilon_{\text{bkg}}(\eta_{\text{jet }i})\epsilon_{\text{bkg}}(\eta_{\text{jet }j}) \right), \tag{6.2}$$

where $N_{0\text{-tag}}$ is the number of zero-tag events in data.

The two background predictions will agree if ϵ_{bkg} is jet- and process-independent. Thus, we use the prediction $N_{\geq 2\text{-tag bkg}}$ as the nominal background prediction, and the difference between the two predictions as an estimate of the systematic uncertainty of the method resulting from any additional process dependence. This systematic uncertainty is found to be 13%.

Events satisfying the nominal MR selection with two misidentified TD jets are used to define a validation region (VR) in order to test the accuracy of the prediction method. Using the ϵ_{bkg} measured in the MR and the same matrix method, we predict 1.1 ± 0.7 background events in the VR and observe 1 event in data. Another validation test is performed by relaxing the jet η requirement to $|\eta| < 1.48$ in order to decrease the statistical uncertainty of the test. For the alternative test, we estimate 5.1 ± 3.1 events in the VR and observe 4 events in data. Both tests produce excellent agreement between the predicted and observed yields, thus validating the background estimation method. Finally, a validation of the η dependence of ϵ_{bkg} is shown in appendix B, where the η distribution of the TD-tagged jets in the one tag bin of the signal region data is observed to agree with the predicted background.

Although the dominant background contribution is from instrumental misidentification, there are small contributions from noncollision sources including cosmic ray muons

JHEP07(2023)210

and beam halo particles. To estimate these contributions, we first measure the efficiencies of the cosmic ray and beam halo vetoes in dedicated MRs with high cosmic ray muon and beam halo purities, respectively. The cosmic ray muon MR is composed of events selected by cosmic ray triggers, enabled during periods when the LHC is not colliding proton beams, and containing a muon that traverses the full detector and a jet. Events in the beam halo MR are selected by an alternative beam halo filter, which identifies beam halo particles via matching segments in the CSC endcap muon detector. For the beam halo MR, we also subtract the instrumental misidentified collision background using the matrix method to prevent the resulting bias on the measured beam halo veto efficiency. Finally, we invert the cosmic ray muon and beam halo vetoes described in section 4.3 to obtain two separate CRs. We multiply the corresponding CR event yields by a transfer factor accounting for the measured efficiency of the cosmic ray muon or beam halo veto. We obtain predictions for the cosmic ray muon and beam halo backgrounds of 0.03 ± 0.02 and 0.05 ± 0.05 events, respectively, consistent with zero events in each case.

7 Systematic uncertainties

The source of the dominant background uncertainty is the estimation of the misidentified TD jet background. This uncertainty includes contributions related to the CR sample size, ϵ_{bkg} process dependence, and the matrix method validity, amounting to 4, 30, and 13%, respectively, relative to the total background prediction. The noncollision background uncertainties correspond to about 23% relative to the total background prediction. Several systematic uncertainties in the signal yield prediction are also considered. The uncertainty in the TD jet tagger efficiency, which includes a component from the jet time correction uncertainty as well as a component estimated using the methods discussed in section 5.1, is the largest and amounts to up to 29% relative to the signal yield, depending on the signal model parameters. The integrated luminosities for the 2016, 2017, and 2018 data-taking years have 1.2–2.5% individual uncertainties [93–95], while the overall uncertainty for the 2016–2018 period is 1.6%. The impact of uncertainties related to jet energy scale and resolution [74, 96], PDFs, missing higher order QCD corrections, pileup modeling, integrated luminosity, simulation sample size, and lepton and photon veto efficiency is also estimated and summarized in table 2.

8 Results and interpretation

Figure 7 shows the observed data for the three bins corresponding to $N_{\text{TDJ}} = 0$, 1, and ≥ 2, and the estimated background yields for the latter two N_{TDJ} bins. In the most sensitive SR bin, corresponding to $N_{\text{TDJ}} \geq 2$, we observe 0 events with an expected background of 0.23 ± 0.10 events.

We interpret the results in the context of a simplified model of GMSB chargino-neutralino production [34, 35]. As discussed in section 1, the long-lived neutralinos are effectively pair produced and decay to either $\text{H}\widetilde{\text{G}}$ or $\text{Z}\widetilde{\text{G}}$. The branching fraction $\mathcal{B}(\widetilde{\chi}_1^0 \to \text{H}\widetilde{\text{G}})$ is varied from 0 to 1, assuming $\mathcal{B}(\widetilde{\chi}_1^0 \to \text{H}\widetilde{\text{G}}) + \mathcal{B}(\widetilde{\chi}_1^0 \to \text{Z}\widetilde{\text{G}}) = 1.0$

JHEP07(2023)210

Uncertainty source	Process	Uncertainty [%]
Background CR sample size	Background	4
TD jet tagger misidentification process dependence	Background	30
Background estimation method	Background	13
Noncollision background	Background	23
TD jet tagger efficiency	Signal	8–29
Jet energy scale	Signal	0.1–11
Jet energy resolution	Signal	0.2–10
PDFs	Signal	$\leq$1
Missing higher-order QCD corrections	Signal	$\leq$1
Pileup	Signal	0.3–6.3
Integrated luminosity	Signal	2.5
Signal sample size	Signal	5–8
Lepton and photon veto efficiency	Signal	$\ll$1

Table 2. Summary of combined statistical and systematic uncertainties, the size of their effect, and whether it applies to the signal or background yield predictions. Ranges for signal systematic uncertainties reflect their impact on different signal parameter space points.

We use a test statistic based on the profile likelihood ratio [97] to extract the signal. Upper limits at 95% confidence level (CL) on the product of the neutralino pair production cross section ($\sigma_{\widetilde{\chi}_1^0\widetilde{\chi}_1^0}$) and the relevant branching fraction are derived using the modified frequentist $\mathrm{CL_s}$ criterion [98, 99] and an asymptotic formulae [100]. Systematic uncertainties are incorporated into the analysis via nuisance parameters with log-normal probability density functions and are treated according to the frequentist paradigm.

Figures 8 and 9 show the upper limits on $\sigma_{\widetilde{\chi}_1^0\widetilde{\chi}_1^0}$ as functions of the $\widetilde{\chi}_1^0$ mass ($m_{\widetilde{\chi}_1^0}$) and proper decay length ($c\tau_{\widetilde{\chi}_1^0}$), respectively, assuming $\mathcal{B}(\widetilde{\chi}_1^0 \to \mathrm{H}\widetilde{\mathrm{G}}) = 0.5$. Figure 10 shows the observed upper limits as a function of both $m_{\widetilde{\chi}_1^0}$ and $c\tau_{\widetilde{\chi}_1^0}$. The upper limits are relatively independent of the branching fraction $\mathcal{B}(\widetilde{\chi}_1^0 \to \mathrm{H}\widetilde{\mathrm{G}})$, varying by less than 10% over the full range. For example, for $c\tau_{\widetilde{\chi}_1^0} = 0.5\,\mathrm{m}$ we exclude cross sections of 160, 2.6, and 0.8 fb for $m_{\widetilde{\chi}_1^0}$ of 200, 400, and 600 GeV, respectively. Compared to previous searches for promptly decaying $\widetilde{\chi}_1^0$ in the same simplified model [101], the sensitivity of the current search expressed in terms of the cross section limit is about 20 (10) times better at $m_{\widetilde{\chi}_1^0} = 400$ (600) GeV. At a 95% CL, we exclude $\widetilde{\chi}_1^0$ masses up to approximately 1180 (990) GeV when $c\tau_{\widetilde{\chi}_1^0}$ is 0.5 (3.0) m. For $m_{\widetilde{\chi}_1^0} = 400$ (1000) GeV, we exclude $c\tau_{\widetilde{\chi}_1^0}$ in the range from 0.04 to 20 (0.1 to 3) m. Tabulated results are provided in the HEPData record for this analysis [36].

JHEP07(2023)210

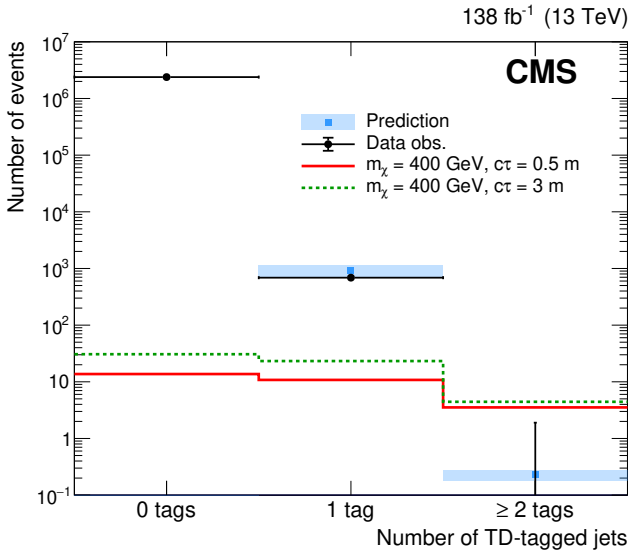

Figure 7. Distribution of the number of TD-tagged jets for the $m_{\widetilde{\chi}_1^0} = 400\,\text{GeV}$ simulated signal samples with $c\tau_{\widetilde{\chi}_1^0} = 0.5\,\text{m}$ (solid red line) and $c\tau_{\widetilde{\chi}_1^0} = 3.0\,\text{m}$ (dotted green line), estimated background (blue square markers), and data (black round markers). The signal distributions are normalized to the expected cross section limit. The blue shaded region indicates the systematic uncertainty in the background prediction. No background prediction is shown for the bin with zero TD-tagged jets as it is the main control region used to predict the background for the other two bins. There are zero observed events in the bin with two or more TD-tagged jets.

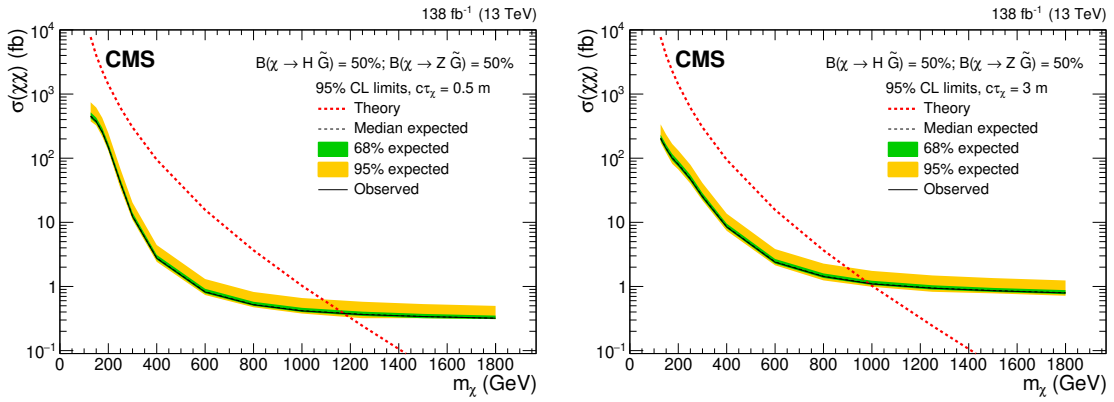

Figure 8. Expected and observed 95% CL upper limits on $\sigma_{\widetilde{\chi}_1^0\widetilde{\chi}_1^0}$ as functions of $m_{\widetilde{\chi}_1^0}$ in a scenario with $\mathcal{B}(\widetilde{\chi}_1^0 \to \text{H}\widetilde{\text{G}}) = 0.5$ and $c\tau = 0.5\,\text{m}$ (left) or 3 m (right).

JHEP07(2023)210

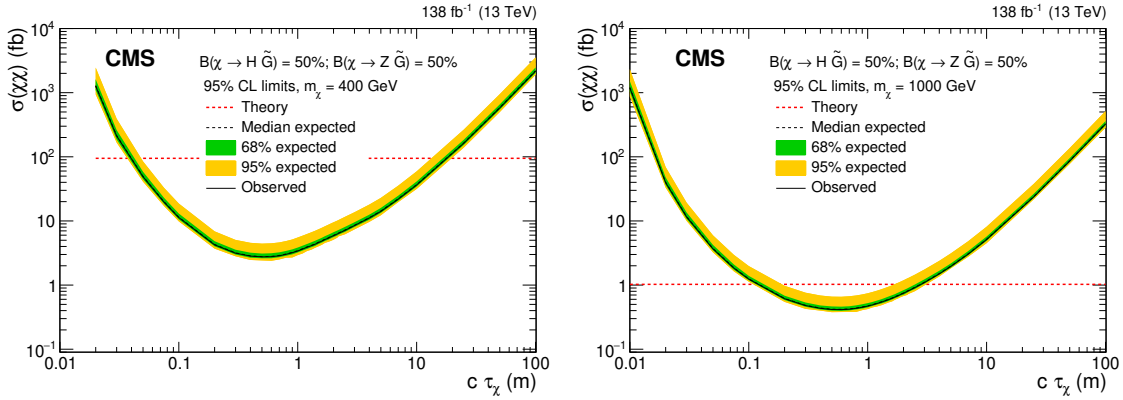

Figure 9. Expected and observed 95% CL upper limits on $\sigma_{\widetilde{\chi}_1^0\widetilde{\chi}_1^0}$ as functions of $c\tau_{\widetilde{\chi}_1^0}$ in a scenario with $\mathcal{B}(\widetilde{\chi}_1^0 \to \mathrm{H}\widetilde{\mathrm{G}}) = 0.5$ and $m_{\widetilde{\chi}_1^0} = 400\,\mathrm{GeV}$ (left) or $1000\,\mathrm{GeV}$ (right).

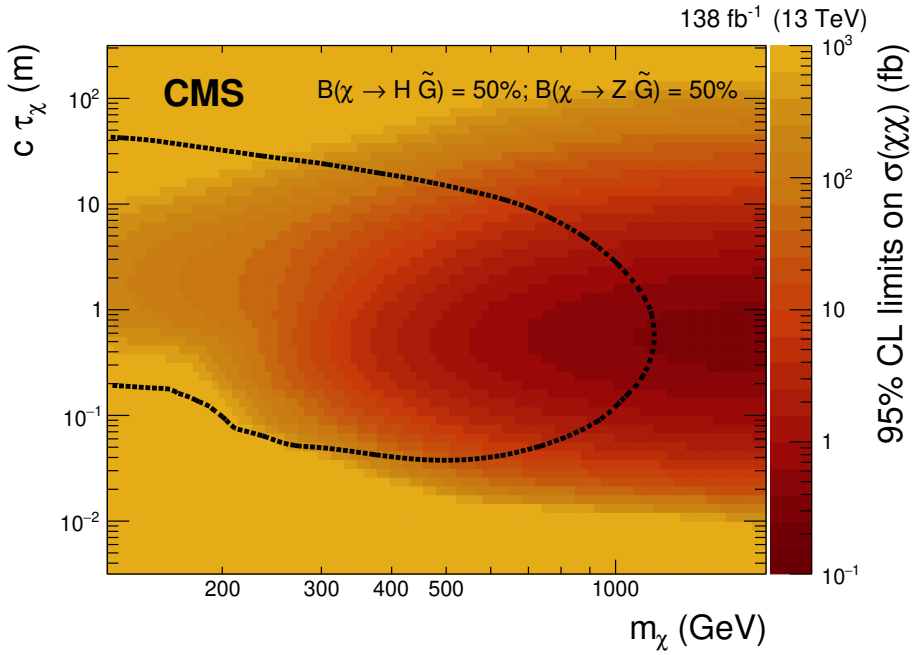

Figure 10. The observed 95% CL upper limit on $\sigma_{\widetilde{\chi}_1^0\widetilde{\chi}_1^0}$ as a function of $m_{\widetilde{\chi}_1^0}$ and $c\tau_{\widetilde{\chi}_1^0}$ in a scenario with $\mathcal{B}(\widetilde{\chi}_1^0 \to \mathrm{H}\widetilde{\mathrm{G}}) = 0.5$. The area enclosed by the dotted black line corresponds to the observed excluded region.

JHEP07(2023)210

9 Summary

A search for long-lived particles has been carried out using proton-proton collision data at $\sqrt{s} = 13\,\text{TeV}$, corresponding to an integrated luminosity of $138\,\text{fb}^{-1}$, using missing transverse momentum and a novel and highly discriminating deep neural network tagger for trackless and delayed (TD) jets. Each additional TD-tagged jet required suppresses standard model background processes by more than three orders of magnitude while maintaining the signal efficiency above 80%. A background estimation method based on control samples in data uses the tagger's measured misidentification probability to extrapolate from event samples with one or fewer tagged jets to the signal region comprising events with two or more tagged jets. The results are interpreted in the context of a simplified model of electroweak production of chargino-neutralino pairs. For a neutralino ($\widetilde{\chi}_1^0$) proper decay length of $c\tau_{\widetilde{\chi}_1^0} = 0.5\,\text{m}$, we exclude cross sections of 160, 2.6, and 0.8 fb for $\widetilde{\chi}_1^0$ masses ($m_{\widetilde{\chi}_1^0}$) of 200, 400, and 600 GeV, respectively, at 95% confidence level. Compared to previous searches for promptly decaying $\widetilde{\chi}_1^0$ in the same simplified model, the sensitivity of the current search expressed in terms of cross section limit is about 20 (10) times better at $m_{\widetilde{\chi}_1^0} = 400\ (600)\,\text{GeV}$. In the case of a long-lived $\widetilde{\chi}_1^0$ with $c\tau_{\widetilde{\chi}_1^0} = 0.5\,\text{m}$, $\widetilde{\chi}_1^0$ masses up to 1.18 TeV are excluded at 95% confidence level. The current search is the best result to date in the mass range from the kinematic limit imposed by the Higgs boson mass up to 1.8 TeV.

Acknowledgments

We congratulate our colleagues in the CERN accelerator departments for the excellent performance of the LHC and thank the technical and administrative staffs at CERN and at other CMS institutes for their contributions to the success of the CMS effort. In addition, we gratefully acknowledge the computing centers and personnel of the Worldwide LHC Computing Grid and other centers for delivering so effectively the computing infrastructure essential to our analyses. Finally, we acknowledge the enduring support for the construction and operation of the LHC, the CMS detector, and the supporting computing infrastructure provided by the following funding agencies: BMBWF and FWF (Austria); FNRS and FWO (Belgium); CNPq, CAPES, FAPERJ, FAPERGS, and FAPESP (Brazil); MES and BNSF (Bulgaria); CERN; CAS, MoST, and NSFC (China); MINCIENCIAS (Colombia); MSES and CSF (Croatia); RIF (Cyprus); SENESCYT (Ecuador); MoER, ERC PUT and ERDF (Estonia); Academy of Finland, MEC, and HIP (Finland); CEA and CNRS/IN2P3 (France); BMBF, DFG, and HGF (Germany); GSRI (Greece); NKFIH (Hungary); DAE and DST (India); IPM (Iran); SFI (Ireland); INFN (Italy); MSIP and NRF (Republic of Korea); MES (Latvia); LAS (Lithuania); MOE and UM (Malaysia); BUAP, CINVESTAV, CONACYT, LNS, SEP, and UASLP-FAI (Mexico); MOS (Montenegro); MBIE (New Zealand); PAEC (Pakistan); MES and NSC (Poland); FCT (Portugal); MESTD (Serbia); MCIN/AEI and PCTI (Spain); MOSTR (Sri Lanka); Swiss Funding Agencies (Switzerland); MST (Taipei); MHESI and NSTDA (Thailand); TUBITAK and TENMAK (Turkey); NASU (Ukraine); STFC (United Kingdom); DOE and NSF (U.S.A.).

JHEP07(2023)210

Individuals have received support from the Marie-Curie program and the European Research Council and Horizon 2020 Grant, contract Nos. 675440, 724704, 752730, 758316, 765710, 824093, 884104, and COST Action CA16108 (European Union); the Leventis Foundation; the Alfred P. Sloan Foundation; the Alexander von Humboldt Foundation; the Belgian Federal Science Policy Office; the Fonds pour la Formation à la Recherche dans l'Industrie et dans l'Agriculture (FRIA-Belgium); the Agentschap voor Innovatie door Wetenschap en Technologie (IWT-Belgium); the F.R.S.-FNRS and FWO (Belgium) under the "Excellence of Science – EOS" – be.h project n. 30820817; the Beijing Municipal Science & Technology Commission, No. Z191100007219010; the Ministry of Education, Youth and Sports (MEYS) of the Czech Republic; the Hellenic Foundation for Research and Innovation (HFRI), Project Number 2288 (Greece); the Deutsche Forschungsgemeinschaft (DFG), under Germany's Excellence Strategy – EXC 2121 "Quantum Universe" – 390833306, and under project number 400140256 — GRK2497; the Hungarian Academy of Sciences, the New National Excellence Program — ÚNKP, the NKFIH research grants K 124845, K 124850, K 128713, K 128786, K 129058, K 131991, K 133046, K 138136, K 143460, K 143477, 2020-2.2.1-ED-2021-00181, and TKP2021-NKTA-64 (Hungary); the Council of Science and Industrial Research, India; the Latvian Council of Science; the Ministry of Education and Science, project no. 2022/WK/14, and the National Science Center, contracts Opus 2021/41/B/ST2/01369 and 2021/43/B/ST2/01552 (Poland); the Fundação para a Ciência e a Tecnologia, grant CEECIND/01334/2018 (Portugal); the National Priorities Research Program by Qatar National Research Fund; MCIN/AEI/10.13039/501100011033, ERDF "a way of making Europe", and the Programa Estatal de Fomento de la Investigación Científica y Técnica de Excelencia María de Maeztu, grant MDM-2017-0765 and Programa Severo Ochoa del Principado de Asturias (Spain); the Chulalongkorn Academic into Its 2nd Century Project Advancement Project, and the National Science, Research and Innovation Fund via the Program Management Unit for Human Resources & Institutional Development, Research and Innovation, grant B05F650021 (Thailand); the Kavli Foundation; the Nvidia Corporation; the SuperMicro Corporation; the Welch Foundation, contract C-1845; and the Weston Havens Foundation (U.S.A.).

JHEP07(2023)210

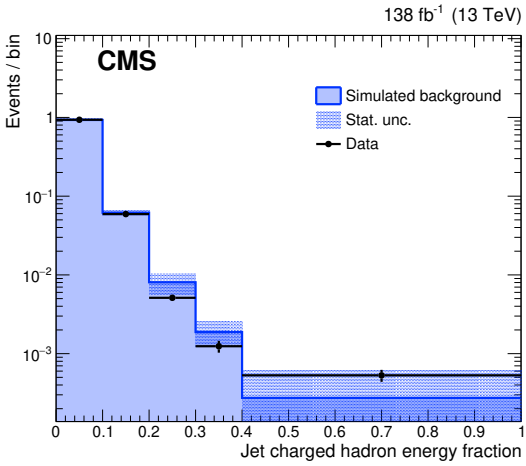

Figure 11. The distribution of the jet charged hadron energy fraction, a variable used as input to the TD jet tagger score, for simulation (shaded histogram) and data (black markers) when using electrons from $W \to e\nu_e$ events as proxy objects for signal jets. The histograms and data points have been normalized to unit area. Similar levels of agreement are observed for photon proxy objects from the $Z \to \ell^+\ell^-\gamma$ sample.

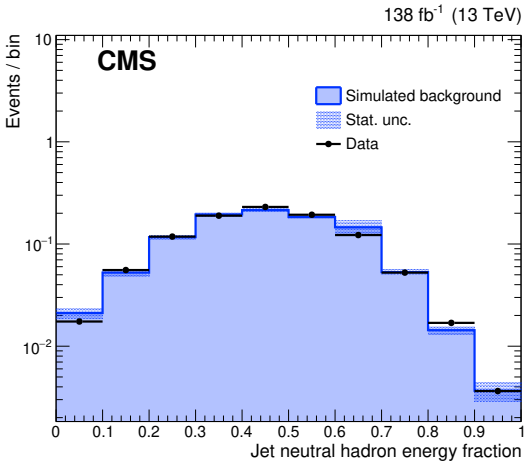

Figure 12. The distribution of the jet neutral hadron energy fraction, a variable used as input to the TD jet tagger score, for simulation (shaded histogram) and data (black markers) when using electrons from $W \to e\nu_e$ events as proxy objects for signal jets. The histograms and data points have been normalized to unit area. Similar levels of agreement are observed for photon proxy objects from the $Z \to \ell^+\ell^-\gamma$ sample.

A Trackless delayed jet tagger input variables

The key input variables to the TD jet tagger are the charged hadron energy fraction, neutral hadron energy fraction, and number of track constituents. Comparisons between the simulation-based predictions and data are shown for these three variables in figures 11, 12, and 13, respectively.

JHEP07(2023)210

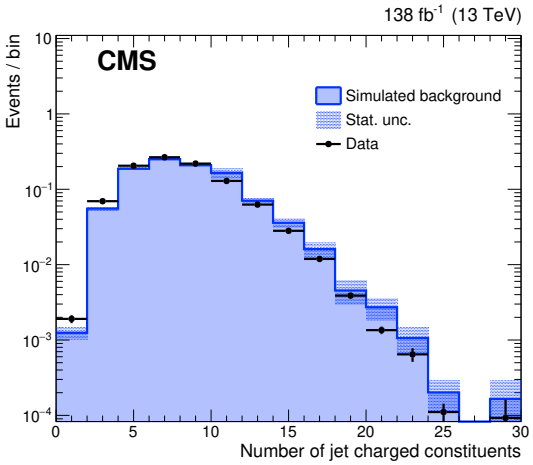

Figure 13. The distribution of the number of track constituents in the jet, a variable used as input to the TD jet tagger score, for simulation (shaded histogram) and data (black markers) when using electrons from $W \to e\nu_e$ events as proxy objects for signal jets. The histograms and data points have been normalized to unit area. Similar levels of agreement are observed for photon proxy objects from the $Z \to \ell^+\ell^-\gamma$ sample.

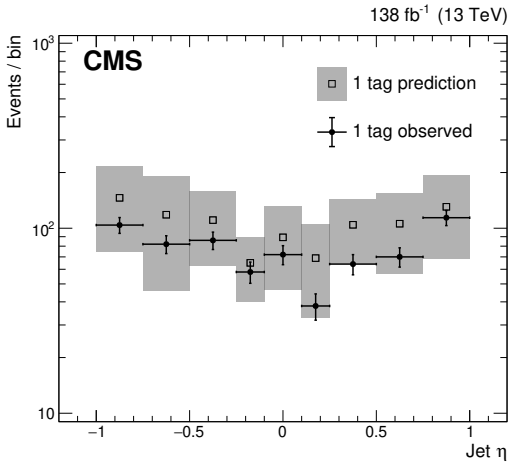

Figure 14. The η distribution of TD-tagged jets in a background-enriched control region that comprises events with exactly one TD-tagged jet. Observed data (black round markers) and the corresponding prediction based on control samples in data (empty squared markers), measured using the nominal W+jets MR, are compared. The prediction uncertainty (gray band) includes the systematic uncertainty quantifying the degree of process dependence measured from alternative MRs. The predictions for the shape and the normalization of the η distribution are consistent with the data.

B TD-tagged jet η distribution

The η distribution of TD-tagged jets in data and the corresponding prediction from the background estimation method are compared in figure 14.

JHEP07(2023)210

References

[1] G.F. Giudice and R. Rattazzi, *Theories with gauge mediated supersymmetry breaking*, *Phys. Rept.* **322** (1999) 419 [hep-ph/9801271] [INSPIRE].

[2] P. Meade, N. Seiberg and D. Shih, *General gauge mediation*, *Prog. Theor. Phys. Suppl.* **177** (2009) 143 [arXiv:0801.3278] [INSPIRE].

[3] M. Buican, P. Meade, N. Seiberg and D. Shih, *Exploring general gauge mediation*, *JHEP* **03** (2009) 016 [arXiv:0812.3668] [INSPIRE].

[4] G.F. Giudice and A. Romanino, *Split supersymmetry*, *Nucl. Phys. B* **699** (2004) 65 [*Erratum ibid.* **706** (2005) 487] [hep-ph/0406088] [INSPIRE].

[5] J.A.L. Hewett, B. Lillie, M. Masip and T.G. Rizzo, *Signatures of long-lived gluinos in split supersymmetry*, *JHEP* **09** (2004) 070 [hep-ph/0408248] [INSPIRE].

[6] N. Arkani-Hamed, S. Dimopoulos, G.F. Giudice and A. Romanino, *Aspects of split supersymmetry*, *Nucl. Phys. B* **709** (2005) 3 [hep-ph/0409232] [INSPIRE].

[7] P. Gambino, G.F. Giudice and P. Slavich, *Gluino decays in split supersymmetry*, *Nucl. Phys. B* **726** (2005) 35 [hep-ph/0506214] [INSPIRE].

[8] A. Arvanitaki, N. Craig, S. Dimopoulos and G. Villadoro, *Mini-split*, *JHEP* **02** (2013) 126 [arXiv:1210.0555] [INSPIRE].

[9] N. Arkani-Hamed et al., *Simply unnatural supersymmetry*, arXiv:1212.6971 [INSPIRE].

[10] P. Fayet, *Supergauge invariant extension of the Higgs mechanism and a model for the electron and its neutrino*, *Nucl. Phys. B* **90** (1975) 104 [INSPIRE].

[11] G.R. Farrar and P. Fayet, *Phenomenology of the production, decay, and detection of new hadronic states associated with supersymmetry*, *Phys. Lett. B* **76** (1978) 575 [INSPIRE].

[12] S. Weinberg, *Supersymmetry at ordinary energies. 1. Masses and conservation laws*, *Phys. Rev. D* **26** (1982) 287 [INSPIRE].

[13] R. Barbier et al., *R-parity violating supersymmetry*, *Phys. Rept.* **420** (2005) 1 [hep-ph/0406039] [INSPIRE].

[14] J.J. Fan, M. Reece and J.T. Ruderman, *Stealth supersymmetry*, *JHEP* **11** (2011) 012 [arXiv:1105.5135] [INSPIRE].

[15] J.J. Fan, M. Reece and J.T. Ruderman, *A stealth supersymmetry sampler*, *JHEP* **07** (2012) 196 [arXiv:1201.4875] [INSPIRE].

[16] M.J. Strassler and K.M. Zurek, *Echoes of a hidden valley at hadron colliders*, *Phys. Lett. B* **651** (2007) 374 [hep-ph/0604261] [INSPIRE].

[17] M.J. Strassler and K.M. Zurek, *Discovering the Higgs through highly-displaced vertices*, *Phys. Lett. B* **661** (2008) 263 [hep-ph/0605193] [INSPIRE].

[18] T. Han, Z. Si, K.M. Zurek and M.J. Strassler, *Phenomenology of hidden valleys at hadron colliders*, *JHEP* **07** (2008) 008 [arXiv:0712.2041] [INSPIRE].

JHEP07(2023)210

[19] Y. Cui, L. Randall and B. Shuve, *A WIMPy baryogenesis miracle*, *JHEP* **04** (2012) 075 [arXiv:1112.2704] [INSPIRE].

[20] Y. Cui and R. Sundrum, *Baryogenesis for weakly interacting massive particles*, *Phys. Rev. D* **87** (2013) 116013 [arXiv:1212.2973] [INSPIRE].

[21] Y. Cui and B. Shuve, *Probing baryogenesis with displaced vertices at the LHC*, *JHEP* **02** (2015) 049 [arXiv:1409.6729] [INSPIRE].

[22] D. Tucker-Smith and N. Weiner, *Inelastic dark matter*, *Phys. Rev. D* **64** (2001) 043502 [hep-ph/0101138] [INSPIRE].

[23] Z. Chacko, H.-S. Goh and R. Harnik, *The twin Higgs: natural electroweak breaking from mirror symmetry*, *Phys. Rev. Lett.* **96** (2006) 231802 [hep-ph/0506256] [INSPIRE].

[24] D. Curtin and C.B. Verhaaren, *Discovering uncolored naturalness in exotic Higgs decays*, *JHEP* **12** (2015) 072 [arXiv:1506.06141] [INSPIRE].

[25] H.-C. Cheng, S. Jung, E. Salvioni and Y. Tsai, *Exotic quarks in twin Higgs models*, *JHEP* **03** (2016) 074 [arXiv:1512.02647] [INSPIRE].

[26] CMS collaboration, *Search for long-lived particles using displaced jets in proton-proton collisions at* $\sqrt{s} = 13$ *TeV*, *Phys. Rev. D* **104** (2021) 012015 [arXiv:2012.01581] [INSPIRE].

[27] ATLAS collaboration, *Search for long-lived, massive particles in events with displaced vertices and missing transverse momentum in* $\sqrt{s} = 13$ *TeV pp collisions with the ATLAS detector*, *Phys. Rev. D* **97** (2018) 052012 [arXiv:1710.04901] [INSPIRE].

[28] ATLAS collaboration, *Search for the Higgs boson produced in association with a vector boson and decaying into two spin-zero particles in the* $H \to aa \to 4b$ *channel in pp collisions at* $\sqrt{s} = 13$ *TeV with the ATLAS detector*, *JHEP* **10** (2018) 031 [arXiv:1806.07355] [INSPIRE].

[29] ATLAS collaboration, *Search for neutral long-lived particles in pp collisions at* $\sqrt{s} = 13$ *TeV that decay into displaced hadronic jets in the ATLAS calorimeter*, *JHEP* **06** (2022) 005 [arXiv:2203.01009] [INSPIRE].

[30] ATLAS collaboration, *Search for exotic decays of the Higgs boson into long-lived particles in pp collisions at* $\sqrt{s} = 13$ *TeV using displaced vertices in the ATLAS inner detector*, *JHEP* **11** (2021) 229 [arXiv:2107.06092] [INSPIRE].

[31] ATLAS collaboration, *Search for events with a pair of displaced vertices from long-lived neutral particles decaying into hadronic jets in the ATLAS muon spectrometer in pp collisions at* $\sqrt{s} = 13$ *TeV*, *Phys. Rev. D* **106** (2022) 032005 [arXiv:2203.00587] [INSPIRE].

[32] CMS collaboration, *Search for long-lived particles decaying in the CMS end cap muon detectors in proton-proton collisions at* $\sqrt{s} = 13$ *TeV*, *Phys. Rev. Lett.* **127** (2021) 261804 [arXiv:2107.04838] [INSPIRE].

[33] CMS collaboration, *Search for long-lived particles using nonprompt jets and missing transverse momentum with proton-proton collisions at* $\sqrt{s} = 13$ *TeV*, *Phys. Lett. B* **797** (2019) 134876 [arXiv:1906.06441] [INSPIRE].

[34] S. Dimopoulos, M. Dine, S. Raby and S.D. Thomas, *Experimental signatures of low-energy gauge mediated supersymmetry breaking*, *Phys. Rev. Lett.* **76** (1996) 3494 [hep-ph/9601367] [INSPIRE].

JHEP07(2023)210

[35] K.T. Matchev and S.D. Thomas, *Higgs and Z boson signatures of supersymmetry*, *Phys. Rev. D* **62** (2000) 077702 [hep-ph/9908482] [INSPIRE].

[36] CMS collaboration, *Search for long-lived particles using out-of-time trackless jets in proton-proton collisions at* $\sqrt{s} = 13$ *TeV*, https://www.hepdata.net/record/ins2613855 [DOI:10.17182/HEPDATA.135827].

[37] CMS collaboration, *Search for long-lived particles using delayed photons in proton-proton collisions at* $\sqrt{s} = 13$ *TeV*, *Phys. Rev. D* **100** (2019) 112003 [arXiv:1909.06166] [INSPIRE].

[38] CMS collaboration, *Performance of the CMS level-1 trigger in proton-proton collisions at* $\sqrt{s} = 13$ *TeV*, 2020 *JINST* **15** P10017 [arXiv:2006.10165] [INSPIRE].

[39] CMS collaboration, *The CMS trigger system*, 2017 *JINST* **12** P01020 [arXiv:1609.02366] [INSPIRE].

[40] CMS collaboration, *The CMS experiment at the CERN LHC*, 2008 *JINST* **3** S08004 [INSPIRE].

[41] J. Alwall et al., *The automated computation of tree-level and next-to-leading order differential cross sections, and their matching to parton shower simulations*, *JHEP* **07** (2014) 079 [arXiv:1405.0301] [INSPIRE].

[42] J. Alwall et al., *Comparative study of various algorithms for the merging of parton showers and matrix elements in hadronic collisions*, *Eur. Phys. J. C* **53** (2008) 473 [arXiv:0706.2569] [INSPIRE].

[43] J. Alwall, S. de Visscher and F. Maltoni, *QCD radiation in the production of heavy colored particles at the LHC*, *JHEP* **02** (2009) 017 [arXiv:0810.5350] [INSPIRE].

[44] R. Gavin, Y. Li, F. Petriello and S. Quackenbush, *FEWZ* 2.0*: a code for hadronic Z production at next-to-next-to-leading order*, *Comput. Phys. Commun.* **182** (2011) 2388 [arXiv:1011.3540] [INSPIRE].

[45] R. Gavin, Y. Li, F. Petriello and S. Quackenbush, *W physics at the LHC with FEWZ* 2.1, *Comput. Phys. Commun.* **184** (2013) 208 [arXiv:1201.5896] [INSPIRE].

[46] M. Czakon and A. Mitov, *Top++: a program for the calculation of the top-pair cross-section at hadron colliders*, *Comput. Phys. Commun.* **185** (2014) 2930 [arXiv:1112.5675] [INSPIRE].

[47] S. Alioli, P. Nason, C. Oleari and E. Re, *NLO single-top production matched with shower in POWHEG: s- and t-channel contributions*, *JHEP* **09** (2009) 111 [*Erratum ibid.* **02** (2010) 011] [arXiv:0907.4076] [INSPIRE].

[48] W. Beenakker, R. Höpker, M. Spira and P.M. Zerwas, *Squark and gluino production at hadron colliders*, *Nucl. Phys. B* **492** (1997) 51 [hep-ph/9610490] [INSPIRE].

[49] A. Kulesza and L. Motyka, *Threshold resummation for squark-antisquark and gluino-pair production at the LHC*, *Phys. Rev. Lett.* **102** (2009) 111802 [arXiv:0807.2405] [INSPIRE].

[50] A. Kulesza and L. Motyka, *Soft gluon resummation for the production of gluino-gluino and squark-antisquark pairs at the LHC*, *Phys. Rev. D* **80** (2009) 095004 [arXiv:0905.4749] [INSPIRE].

[51] W. Beenakker et al., *Soft-gluon resummation for squark and gluino hadroproduction*, *JHEP* **12** (2009) 041 [arXiv:0909.4418] [INSPIRE].

JHEP07(2023)210

[52] W. Beenakker et al., *Squark and gluino hadroproduction*, *Int. J. Mod. Phys. A* **26** (2011) 2637 [arXiv:1105.1110] [INSPIRE].

[53] C. Borschensky et al., *Squark and gluino production cross sections in pp collisions at* $\sqrt{s} = 13$, 14, 33 *and* 100 *TeV*, *Eur. Phys. J. C* **74** (2014) 3174 [arXiv:1407.5066] [INSPIRE].

[54] B. Fuks, M. Klasen, D.R. Lamprea and M. Rothering, *Precision predictions for electroweak superpartner production at hadron colliders with Resummino*, *Eur. Phys. J. C* **73** (2013) 2480 [arXiv:1304.0790] [INSPIRE].

[55] B. Fuks, M. Klasen, D.R. Lamprea and M. Rothering, *Gaugino production in proton-proton collisions at a center-of-mass energy of* 8 *TeV*, *JHEP* **10** (2012) 081 [arXiv:1207.2159] [INSPIRE].

[56] P.Z. Skands et al., *SUSY Les Houches accord: interfacing SUSY spectrum calculators, decay packages, and event generators*, *JHEP* **07** (2004) 036 [hep-ph/0311123] [INSPIRE].

[57] CMS collaboration, *Combined search for electroweak production of charginos and neutralinos in proton-proton collisions at* $\sqrt{s} = 13$ *TeV*, *JHEP* **03** (2018) 160 [arXiv:1801.03957] [INSPIRE].

[58] CMS collaboration, *Search for supersymmetry with Higgs boson to diphoton decays using the razor variables at* $\sqrt{s} = 13$ *TeV*, *Phys. Lett. B* **779** (2018) 166 [arXiv:1709.00384] [INSPIRE].

[59] NNPDF collaboration, *Parton distributions for the LHC Run II*, *JHEP* **04** (2015) 040 [arXiv:1410.8849] [INSPIRE].

[60] NNPDF collaboration, *Parton distributions from high-precision collider data*, *Eur. Phys. J. C* **77** (2017) 663 [arXiv:1706.00428] [INSPIRE].

[61] T. Sjöstrand et al., *An introduction to PYTHIA* 8.2, *Comput. Phys. Commun.* **191** (2015) 159 [arXiv:1410.3012] [INSPIRE].

[62] CMS collaboration, *Event generator tunes obtained from underlying event and multiparton scattering measurements*, *Eur. Phys. J. C* **76** (2016) 155 [arXiv:1512.00815] [INSPIRE].

[63] CMS collaboration, *Extraction and validation of a new set of CMS PYTHIA*8 *tunes from underlying-event measurements*, *Eur. Phys. J. C* **80** (2020) 4 [arXiv:1903.12179] [INSPIRE].

[64] GEANT4 collaboration, *GEANT*4 — *a simulation toolkit*, *Nucl. Instrum. Meth. A* **506** (2003) 250 [INSPIRE].

[65] CMS collaboration, *Particle-flow reconstruction and global event description with the CMS detector*, 2017 *JINST* **12** P10003 [arXiv:1706.04965] [INSPIRE].

[66] CMS collaboration, *Performance of photon reconstruction and identification with the CMS detector in proton-proton collisions at* $\sqrt{s} = 8$ *TeV*, 2015 *JINST* **10** P08010 [arXiv:1502.02702] [INSPIRE].

[67] CMS collaboration, *Electron and photon reconstruction and identification with the CMS experiment at the CERN LHC*, 2021 *JINST* **16** P05014 [arXiv:2012.06888] [INSPIRE].

[68] CMS collaboration, *ECAL* 2016 *refined calibration and Run*2 *summary plots*, CMS-DP-2020-021, CERN, Geneva, Switzerland (2020).

JHEP07(2023)210

[69] CMS collaboration, *Reconstruction and identification of τ lepton decays to hadrons and ν_τ at CMS*, 2016 *JINST* **11** P01019 [arXiv:1510.07488] [INSPIRE].

[70] CMS collaboration, *Performance of reconstruction and identification of τ leptons decaying to hadrons and ν_τ in pp collisions at $\sqrt{s} = 13$ TeV*, 2018 *JINST* **13** P10005 [arXiv:1809.02816] [INSPIRE].

[71] M. Cacciari, G.P. Salam and G. Soyez, *The anti-k_t jet clustering algorithm*, *JHEP* **04** (2008) 063 [arXiv:0802.1189] [INSPIRE].

[72] M. Cacciari, G.P. Salam and G. Soyez, *FastJet user manual*, *Eur. Phys. J. C* **72** (2012) 1896 [arXiv:1111.6097] [INSPIRE].

[73] CMS collaboration, *Jet energy scale and resolution in the CMS experiment in pp collisions at 8 TeV*, 2017 *JINST* **12** P02014 [arXiv:1607.03663] [INSPIRE].

[74] CMS collaboration, *Performance of missing transverse momentum reconstruction in proton-proton collisions at $\sqrt{s} = 13$ TeV using the CMS detector*, 2019 *JINST* **14** P07004 [arXiv:1903.06078] [INSPIRE].

[75] D. Contardo et al., *Technical proposal for the phase-II upgrade of the CMS detector*, CERN-LHCC-2015-010, CERN, Geneva, Switzerland (2015) [DOI:10.17181/CERN.VU8I.D59J].

[76] CMS collaboration, *Time reconstruction and performance of the CMS electromagnetic calorimeter*, 2010 *JINST* **5** T03011 [arXiv:0911.4044] [INSPIRE].

[77] D. del Re, *Timing performance of the CMS ECAL and prospects for the future*, *J. Phys. Conf. Ser.* **587** (2015) 012003 [INSPIRE].

[78] Particle Data Group collaboration, *Review of particle physics*, *PTEP* **2022** (2022) 083C01 [INSPIRE].

[79] CMS collaboration, *Description and performance of track and primary-vertex reconstruction with the CMS tracker*, 2014 *JINST* **9** P10009 [arXiv:1405.6569] [INSPIRE].

[80] M. Ester, H.-P. Kriegel, J. Sander and X. Xu, *A density-based algorithm for discovering clusters in large spatial databases with noise*, in the proceedings of the *Proc. of the 2nd Int. Conf. on Knowledge Discovery and Data Mining*, (1996), p. 226.

[81] CMS collaboration, *Performance of quark/gluon discrimination in 8 TeV pp data*, CMS-PAS-JME-13-002, CERN, Geneva, Switzerland (2013).

[82] F. Chollet et al., *Keras*, https://keras.io.

[83] M. Abadi et al., *TensorFlow: large-scale machine learning on heterogeneous distributed systems*, arXiv:1603.04467 [INSPIRE].

[84] V. Nair and G.E. Hinton, *Rectified linear units improve restricted Boltzmann machines*, in *Proc. of the 27th Int. Conf. on Machine Learning (ICML)*, (2010), p. 807.

[85] X. Glorot, A. Bordes and Y. Bengio, *Deep sparse rectifier neural networks*, in *Proc. of the 14th Int. Conf. on Artificial Intelligence and Statistics (AISTATS)* **15**, (2011), p. 315.

[86] J.S. Bridle, *Probabilistic interpretation of feedforward classification network outputs, with relationships to statistical pattern recognition*, in *Neurocomputing*, Springer, Berlin, Heidelberg, Germany (1990), p. 227 [DOI:10.1007/978-3-642-76153-9_28].

[87] J.S. Bridle, *Training stochastic model recognition algorithms as networks can lead to maximum mutual information estimation of parameters*, in the proceedings of the *Advances in neural information processing systems*, (1989), p. 211.

JHEP07(2023)210

[88] N. Srivastava et al., *Dropout: a simple way to prevent neural networks from overfitting*, *J. Mach. Learn. Res.* **15** (2014) 1929.

[89] D.P. Kingma and J. Ba, *Adam: a method for stochastic optimization*, in 3rd *Int. Conf. on Learning Representations (ICLR), Conference Track Proc.*, Y. Bengio and Y. LeCun eds., (2015) [arXiv:1412.6980] [INSPIRE].

[90] ATLAS collaboration, *Measurement of the top quark-pair production cross section with ATLAS in pp collisions at* $\sqrt{s} = 7$ *TeV*, *Eur. Phys. J. C* **71** (2011) 1577 [arXiv:1012.1792] [INSPIRE].

[91] CMS collaboration, *Measurement of the* $t\bar{t}$ *production cross section in the dilepton channel in pp collisions at* $\sqrt{s} = 7$ *TeV*, *JHEP* **11** (2012) 067 [arXiv:1208.2671] [INSPIRE].

[92] CMS collaboration, *Performance of the reconstruction and identification of high-momentum muons in proton-proton collisions at* $\sqrt{s} = 13$ *TeV*, 2020 *JINST* **15** P02027 [arXiv:1912.03516] [INSPIRE].

[93] CMS collaboration, *Precision luminosity measurement in proton-proton collisions at* $\sqrt{s} = 13$ *TeV in* 2015 *and* 2016 *at CMS*, *Eur. Phys. J. C* **81** (2021) 800 [arXiv:2104.01927] [INSPIRE].

[94] CMS collaboration, *CMS luminosity measurement for the* 2017 *data-taking period at* $\sqrt{s} = 13$ *TeV*, CMS-PAS-LUM-17-004, CERN, Geneva, Switzerland (2018).

[95] CMS collaboration, *CMS luminosity measurement for the* 2018 *data-taking period at* $\sqrt{s} = 13$ *TeV*, CMS-PAS-LUM-18-002, CERN, Geneva, Switzerland (2019).

[96] CMS collaboration, *Jet algorithms performance in* 13 *TeV data*, CMS-PAS-JME-16-003, CERN, Geneva, Switzerland (2017).

[97] ATLAS, CMS and LHC Higgs Combination Group collaborations, *Procedure for the LHC Higgs boson search combination in Summer* 2011, CMS-NOTE-2011-005, CERN, Geneva, Switzerland (2011).

[98] T. Junk, *Confidence level computation for combining searches with small statistics*, *Nucl. Instrum. Meth. A* **434** (1999) 435 [hep-ex/9902006] [INSPIRE].

[99] A.L. Read, *Presentation of search results: the* CL_s *technique*, *J. Phys. G* **28** (2002) 2693 [INSPIRE].

[100] G. Cowan, K. Cranmer, E. Gross and O. Vitells, *Asymptotic formulae for likelihood-based tests of new physics*, *Eur. Phys. J. C* **71** (2011) 1554 [*Erratum ibid.* **73** (2013) 2501] [arXiv:1007.1727] [INSPIRE].

[101] CMS collaboration, *Search for Higgsino pair production in pp collisions at* $\sqrt{s} = 13$ *TeV in final states with large missing transverse momentum and two Higgs bosons decaying via* $H \to b\bar{b}$, *Phys. Rev. D* **97** (2018) 032007 [arXiv:1709.04896] [INSPIRE].

JHEP07(2023)210

The CMS collaboration

Yerevan Physics Institute, Yerevan, Armenia

A. Tumasyan[1]

Institut für Hochenergiephysik, Vienna, Austria

W. Adam, J.W. Andrejkovic, T. Bergauer, S. Chatterjee, K. Damanakis, M. Dragicevic, A. Escalante Del Valle, P.S. Hussain, M. Jeitler[2], N. Krammer, L. Lechner, D. Liko, I. Mikulec, P. Paulitsch, J. Schieck[2], R. Schöfbeck, D. Schwarz, M. Sonawane, S. Templ, W. Waltenberger, C.-E. Wulz[2]

Universiteit Antwerpen, Antwerpen, Belgium

M.R. Darwish[3], T. Janssen, T. Kello[4], H. Rejeb Sfar, P. Van Mechelen

Vrije Universiteit Brussel, Brussel, Belgium

E.S. Bols, J. D'Hondt, A. De Moor, M. Delcourt, H. El Faham, S. Lowette, A. Morton, D. Müller, A.R. Sahasransu, S. Tavernier, W. Van Doninck, S. Van Putte, D. Vannerom

Université Libre de Bruxelles, Bruxelles, Belgium

B. Clerbaux, G. De Lentdecker, L. Favart, D. Hohov, J. Jaramillo, K. Lee, M. Mahdavikhorrami, I. Makarenko, A. Malara, S. Paredes, L. Pétré, N. Postiau, L. Thomas, M. Vanden Bemden, C. Vander Velde, P. Vanlaer

Ghent University, Ghent, Belgium

D. Dobur, J. Knolle, L. Lambrecht, G. Mestdach, C. Rendón, A. Samalan, K. Skovpen, M. Tytgat, N. Van Den Bossche, B. Vermassen, L. Wezenbeek

Université Catholique de Louvain, Louvain-la-Neuve, Belgium

A. Benecke, G. Bruno, F. Bury, C. Caputo, P. David, C. Delaere, I.S. Donertas, A. Giammanco, K. Jaffel, Sa. Jain, V. Lemaitre, K. Mondal, A. Taliercio, T.T. Tran, P. Vischia, S. Wertz

Centro Brasileiro de Pesquisas Fisicas, Rio de Janeiro, Brazil

G.A. Alves, E. Coelho, C. Hensel, A. Moraes, P. Rebello Teles

Universidade do Estado do Rio de Janeiro, Rio de Janeiro, Brazil

W.L. Aldá Júnior, M. Alves Gallo Pereira, M. Barroso Ferreira Filho, H. Brandao Malbouisson, W. Carvalho, J. Chinellato[5], E.M. Da Costa, G.G. Da Silveira[6], D. De Jesus Damiao, V. Dos Santos Sousa, S. Fonseca De Souza, J. Martins[7], C. Mora Herrera, K. Mota Amarilo, L. Mundim, H. Nogima, A. Santoro, S.M. Silva Do Amaral, A. Sznajder, M. Thiel, A. Vilela Pereira

JHEP07(2023)210

Universidade Estadual Paulista, Universidade Federal do ABC, São Paulo, Brazil
C.A. Bernardes[6], L. Calligaris, T.R. Fernandez Perez Tomei, E.M. Gregores, P.G. Mercadante, S.F. Novaes, Sandra S. Padula

Institute for Nuclear Research and Nuclear Energy, Bulgarian Academy of Sciences, Sofia, Bulgaria
A. Aleksandrov, G. Antchev, R. Hadjiiska, P. Iaydjiev, M. Misheva, M. Rodozov, M. Shopova, G. Sultanov

University of Sofia, Sofia, Bulgaria
A. Dimitrov, T. Ivanov, L. Litov, B. Pavlov, P. Petkov, A. Petrov, E. Shumka

Instituto De Alta Investigación, Universidad de Tarapacá, Casilla 7 D, Arica, Chile
S. Thakur

Beihang University, Beijing, China
T. Cheng, T. Javaid[8], M. Mittal, L. Yuan

Department of Physics, Tsinghua University, Beijing, China
M. Ahmad, G. Bauer[9], Z. Hu, S. Lezki, K. Yi[9,10]

Institute of High Energy Physics, Beijing, China
G.M. Chen[8], H.S. Chen[8], M. Chen[8], F. Iemmi, C.H. Jiang, A. Kapoor, H. Liao, Z.-A. Liu[11], V. Milosevic, F. Monti, R. Sharma, J. Tao, J. Thomas-Wilsker, J. Wang, H. Zhang, J. Zhao

State Key Laboratory of Nuclear Physics and Technology, Peking University, Beijing, China
A. Agapitos, Y. An, Y. Ban, A. Levin, C. Li, Q. Li, X. Lyu, Y. Mao, S.J. Qian, X. Sun, D. Wang, J. Xiao, H. Yang

Sun Yat-Sen University, Guangzhou, China
M. Lu, Z. You

University of Science and Technology of China, Hefei, China
N. Lu

Institute of Modern Physics and Key Laboratory of Nuclear Physics and Ion-beam Application (MOE) — Fudan University, Shanghai, China
X. Gao[4], D. Leggat, H. Okawa, Y. Zhang

Zhejiang University, Hangzhou, Zhejiang, China
Z. Lin, C. Lu, M. Xiao

JHEP07(2023)210

Universidad de Los Andes, Bogota, Colombia
C. Avila, D.A. Barbosa Trujillo, A. Cabrera, C. Florez, J. Fraga

Universidad de Antioquia, Medellin, Colombia
J. Mejia Guisao, F. Ramirez, M. Rodriguez, J.D. Ruiz Alvarez

University of Split, Faculty of Electrical Engineering, Mechanical Engineering and Naval Architecture, Split, Croatia
D. Giljanovic, N. Godinovic, D. Lelas, I. Puljak

University of Split, Faculty of Science, Split, Croatia
Z. Antunovic, M. Kovac, T. Sculac

Institute Rudjer Boskovic, Zagreb, Croatia
V. Brigljevic, B.K. Chitroda, D. Ferencek, S. Mishra, M. Roguljic, A. Starodumov[12], T. Susa

University of Cyprus, Nicosia, Cyprus
A. Attikis, K. Christoforou, S. Konstantinou, J. Mousa, C. Nicolaou, F. Ptochos, P.A. Razis, H. Rykaczewski, H. Saka, A. Stepennov

Charles University, Prague, Czech Republic
M. Finger[12], M. Finger Jr.[12], A. Kveton

Escuela Politecnica Nacional, Quito, Ecuador
E. Ayala

Universidad San Francisco de Quito, Quito, Ecuador
E. Carrera Jarrin

Academy of Scientific Research and Technology of the Arab Republic of Egypt, Egyptian Network of High Energy Physics, Cairo, Egypt
H. Abdalla[13], Y. Assran[14,15]

Center for High Energy Physics (CHEP-FU), Fayoum University, El-Fayoum, Egypt
M. Abdullah Al-Mashad, M.A. Mahmoud

National Institute of Chemical Physics and Biophysics, Tallinn, Estonia
S. Bhowmik, R.K. Dewanjee, K. Ehataht, M. Kadastik, T. Lange, S. Nandan, C. Nielsen, J. Pata, M. Raidal, L. Tani, C. Veelken

Department of Physics, University of Helsinki, Helsinki, Finland
P. Eerola, H. Kirschenmann, K. Osterberg, M. Voutilainen

JHEP07(2023)210

Helsinki Institute of Physics, Helsinki, Finland
S. Bharthuar, E. Brücken, F. Garcia, J. Havukainen, M.S. Kim, R. Kinnunen, T. Lampén, K. Lassila-Perini, S. Lehti, T. Lindén, M. Lotti, L. Martikainen, M. Myllymäki, M.m. Rantanen, H. Siikonen, E. Tuominen, J. Tuominiemi

Lappeenranta-Lahti University of Technology, Lappeenranta, Finland
P. Luukka, H. Petrow, T. Tuuva[†]

IRFU, CEA, Université Paris-Saclay, Gif-sur-Yvette, France
C. Amendola, M. Besancon, F. Couderc, M. Dejardin, D. Denegri, J.L. Faure, F. Ferri, S. Ganjour, P. Gras, G. Hamel de Monchenault, V. Lohezic, J. Malcles, J. Rander, A. Rosowsky, M.Ö. Sahin, A. Savoy-Navarro[16], P. Simkina, M. Titov

Laboratoire Leprince-Ringuet, CNRS/IN2P3, Ecole Polytechnique, Institut Polytechnique de Paris, Palaiseau, France
C. Baldenegro Barrera, F. Beaudette, A. Buchot Perraguin, P. Busson, A. Cappati, C. Charlot, F. Damas, O. Davignon, B. Diab, G. Falmagne, B.A. Fontana Santos Alves, S. Ghosh, R. Granier de Cassagnac, A. Hakimi, B. Harikrishnan, G. Liu, J. Motta, M. Nguyen, C. Ochando, L. Portales, R. Salerno, U. Sarkar, J.B. Sauvan, Y. Sirois, A. Tarabini, E. Vernazza, A. Zabi, A. Zghiche

Université de Strasbourg, CNRS, IPHC UMR 7178, Strasbourg, France
J.-L. Agram[17], J. Andrea, D. Apparu, D. Bloch, G. Bourgatte, J.-M. Brom, E.C. Chabert, C. Collard, D. Darej, U. Goerlach, C. Grimault, A.-C. Le Bihan, P. Van Hove

Institut de Physique des 2 Infinis de Lyon (IP2I), Villeurbanne, France
S. Beauceron, B. Blancon, G. Boudoul, A. Carle, N. Chanon, J. Choi, D. Contardo, P. Depasse, C. Dozen[18], H. El Mamouni, J. Fay, S. Gascon, M. Gouzevitch, G. Grenier, B. Ille, I.B. Laktineh, M. Lethuillier, L. Mirabito, S. Perries, L. Torterotot, M. Vander Donckt, P. Verdier, S. Viret

Georgian Technical University, Tbilisi, Georgia
D. Chokheli, I. Lomidze, Z. Tsamalaidze[12]

RWTH Aachen University, I. Physikalisches Institut, Aachen, Germany
V. Botta, L. Feld, K. Klein, M. Lipinski, D. Meuser, A. Pauls, N. Röwert, M. Teroerde

RWTH Aachen University, III. Physikalisches Institut A, Aachen, Germany
S. Diekmann, A. Dodonova, N. Eich, D. Eliseev, M. Erdmann, P. Fackeldey, D. Fasanella, B. Fischer, T. Hebbeker, K. Hoepfner, F. Ivone, M.y. Lee, L. Mastrolorenzo, M. Merschmeyer, A. Meyer, S. Mondal, S. Mukherjee, D. Noll, A. Novak, F. Nowotny, A. Pozdnyakov, Y. Rath, W. Redjeb, H. Reithler, A. Schmidt,

JHEP07(2023)210

S.C. Schuler, A. Sharma, A. Stein, F. Torres Da Silva De Araujo[19], L. Vigilante, S. Wiedenbeck, S. Zaleski

RWTH Aachen University, III. Physikalisches Institut B, Aachen, Germany

C. Dziwok, G. Flügge, W. Haj Ahmad[20], O. Hlushchenko, T. Kress, A. Nowack, O. Pooth, A. Stahl, T. Ziemons, A. Zotz

Deutsches Elektronen-Synchrotron, Hamburg, Germany

H. Aarup Petersen, M. Aldaya Martin, J. Alimena, P. Asmuss, S. Baxter, M. Bayatmakou, H. Becerril Gonzalez, O. Behnke, A. Bermúdez Martínez, S. Bhattacharya, F. Blekman[21], K. Borras[22], D. Brunner, A. Campbell, A. Cardini, C. Cheng, F. Colombina, S. Consuegra Rodríguez, G. Correia Silva, M. De Silva, G. Eckerlin, D. Eckstein, L.I. Estevez Banos, O. Filatov, E. Gallo[21], A. Geiser, A. Giraldi, G. Greau, A. Grohsjean, V. Guglielmi, M. Guthoff, A. Jafari[23], N.Z. Jomhari, B. Kaech, M. Kasemann, H. Kaveh, C. Kleinwort, R. Kogler, M. Komm, D. Krücker, W. Lange, D. Leyva Pernia, K. Lipka[24], W. Lohmann[25], R. Mankel, I.-A. Melzer-Pellmann, M. Mendizabal Morentin, J. Metwally, A.B. Meyer, G. Milella, M. Mormile, A. Mussgiller, A. Nürnberg, Y. Otarid, D. Pérez Adán, E. Ranken, A. Raspereza, B. Ribeiro Lopes, J. Rübenach, A. Saggio, M. Savitskyi, M. Scham[26,22], V. Scheurer, S. Schnake[22], P. Schütze, C. Schwanenberger[21], M. Shchedrolosiev, R.E. Sosa Ricardo, D. Stafford, N. Tonon[†], M. Van De Klundert, F. Vazzoler, A. Ventura Barroso, R. Walsh, D. Walter, Q. Wang, Y. Wen, K. Wichmann, L. Wiens[22], C. Wissing, S. Wuchterl, Y. Yang, A. Zimermmane Castro Santos

University of Hamburg, Hamburg, Germany

A. Albrecht, S. Albrecht, M. Antonello, S. Bein, L. Benato, M. Bonanomi, P. Connor, K. De Leo, M. Eich, K. El Morabit, F. Feindt, A. Fröhlich, C. Garbers, E. Garutti, M. Hajheidari, J. Haller, A. Hinzmann, H.R. Jabusch, G. Kasieczka, P. Keicher, R. Klanner, W. Korcari, T. Kramer, V. Kutzner, F. Labe, J. Lange, A. Lobanov, C. Matthies, A. Mehta, L. Moureaux, M. Mrowietz, A. Nigamova, Y. Nissan, A. Paasch, K.J. Pena Rodriguez, T. Quadfasel, M. Rieger, O. Rieger, D. Savoiu, J. Schindler, P. Schleper, M. Schröder, J. Schwandt, M. Sommerhalder, H. Stadie, G. Steinbrück, A. Tews, M. Wolf

Karlsruher Institut fuer Technologie, Karlsruhe, Germany

S. Brommer, M. Burkart, E. Butz, T. Chwalek, A. Dierlamm, A. Droll, N. Faltermann, M. Giffels, J.O. Gosewisch, A. Gottmann, F. Hartmann[27], M. Horzela, U. Husemann, M. Klute, R. Koppenhöfer, M. Link, A. Lintuluoto, S. Maier, S. Mitra, Th. Müller, M. Neukum, M. Oh, G. Quast, K. Rabbertz, J. Rauser, I. Shvetsov, H.J. Simonis, N. Trevisani, R. Ulrich, J. van der Linden, R.F. Von Cube, M. Wassmer, S. Wieland, R. Wolf, S. Wozniewski, S. Wunsch, X. Zuo

JHEP07(2023)210

Institute of Nuclear and Particle Physics (INPP), NCSR Demokritos, Aghia Paraskevi, Greece

G. Anagnostou, P. Assiouras, G. Daskalakis, A. Kyriakis, A. Stakia

National and Kapodistrian University of Athens, Athens, Greece

M. Diamantopoulou, D. Karasavvas, P. Kontaxakis, A. Manousakis-Katsikakis, A. Panagiotou, I. Papavergou, N. Saoulidou, K. Theofilatos, E. Tziaferi, K. Vellidis, I. Zisopoulos

National Technical University of Athens, Athens, Greece

G. Bakas, T. Chatzistavrou, G. Karapostoli, K. Kousouris, I. Papakrivopoulos, G. Tsipolitis, A. Zacharopoulou

University of Ioánnina, Ioánnina, Greece

K. Adamidis, I. Bestintzanos, I. Evangelou, C. Foudas, P. Gianneios, C. Kamtsikis, P. Katsoulis, P. Kokkas, P.G. Kosmoglou Kioseoglou, N. Manthos, I. Papadopoulos, J. Strologas

MTA-ELTE Lendület CMS Particle and Nuclear Physics Group, Eötvös Loránd University, Budapest, Hungary

M. Csanád, K. Farkas, M.M.A. Gadallah[28], S. Lökös[29], P. Major, K. Mandal, G. Pásztor, A.J. Rádl[30], O. Surányi, G.I. Veres

Wigner Research Centre for Physics, Budapest, Hungary

M. Bartók[31], G. Bencze, C. Hajdu, D. Horvath[32,33], F. Sikler, V. Veszpremi

Institute of Nuclear Research ATOMKI, Debrecen, Hungary

N. Beni, S. Czellar, J. Karancsi[31], J. Molnar, Z. Szillasi, D. Teyssier

Institute of Physics, University of Debrecen, Debrecen, Hungary

P. Raics, B. Ujvari[34], G. Zilizi

Karoly Robert Campus, MATE Institute of Technology, Gyongyos, Hungary

T. Csorgo[30], F. Nemes[30], T. Novak

Panjab University, Chandigarh, India

J. Babbar, S. Bansal, S.B. Beri, V. Bhatnagar, G. Chaudhary, S. Chauhan, N. Dhingra[35], R. Gupta, A. Kaur, A. Kaur, H. Kaur, M. Kaur, S. Kumar, P. Kumari, M. Meena, K. Sandeep, T. Sheokand, J.B. Singh[36], A. Singla, A. K. Virdi

University of Delhi, Delhi, India

A. Ahmed, A. Bhardwaj, A. Chhetri, B.C. Choudhary, A. Kumar, M. Naimuddin, K. Ranjan, S. Saumya

Saha Institute of Nuclear Physics, HBNI, Kolkata, India

S. Baradia, S. Barman[37], S. Bhattacharya, D. Bhowmik, S. Dutta, S. Dutta, B. Gomber[38], M. Maity[37], P. Palit, G. Saha, B. Sahu, S. Sarkar

JHEP07(2023)210

Indian Institute of Technology Madras, Madras, India
P.K. Behera, S.C. Behera, S. Chatterjee, P. Kalbhor, J.R. Komaragiri[39], D. Kumar[39], A. Muhammad, L. Panwar[39], R. Pradhan, P.R. Pujahari, N.R. Saha, A. Sharma, A.K. Sikdar, S. Verma

Bhabha Atomic Research Centre, Mumbai, India
K. Naskar[40]

Tata Institute of Fundamental Research-A, Mumbai, India
T. Aziz, I. Das, S. Dugad, M. Kumar, G.B. Mohanty, P. Suryadevara

Tata Institute of Fundamental Research-B, Mumbai, India
S. Banerjee, M. Guchait, S. Karmakar, S. Kumar, G. Majumder, K. Mazumdar, S. Mukherjee, A. Thachayath

National Institute of Science Education and Research, An OCC of Homi Bhabha National Institute, Bhubaneswar, Odisha, India
S. Bahinipati[41], A.K. Das, C. Kar, P. Mal, T. Mishra, V.K. Muraleedharan Nair Bindhu[42], A. Nayak[42], P. Saha, S.K. Swain, D. Vats[42]

Indian Institute of Science Education and Research (IISER), Pune, India
A. Alpana, S. Dube, B. Kansal, A. Laha, S. Pandey, A. Rastogi, S. Sharma

Isfahan University of Technology, Isfahan, Iran
H. Bakhshiansohi[43,44], E. Khazaie[44], M. Zeinali[45]

Institute for Research in Fundamental Sciences (IPM), Tehran, Iran
S. Chenarani[46], S.M. Etesami, M. Khakzad, M. Mohammadi Najafabadi

University College Dublin, Dublin, Ireland
M. Grunewald

INFN Sezione di Bari[a], Università di Bari[b], Politecnico di Bari[c], Bari, Italy
M. Abbrescia[a,b], R. Aly[a,c,47], C. Aruta[a,b], A. Colaleo[a], D. Creanza[a,c], L. Cristella[a,b], N. De Filippis[a,c], M. De Palma[a,b], A. Di Florio[a,b], W. Elmetenawee[a,b], F. Errico[a,b], L. Fiore[a], G. Iaselli[a,c], G. Maggi[a,c], M. Maggi[a], I. Margjeka[a,b], V. Mastrapasqua[a,b], S. My[a,b], S. Nuzzo[a,b], A. Pellecchia[a,b], A. Pompili[a,b], G. Pugliese[a,c], R. Radogna[a], D. Ramos[a], A. Ranieri[a], G. Selvaggi[a,b], L. Silvestris[a], F.M. Simone[a,b], Ü. Sözbilir[a], A. Stamerra[a], R. Venditti[a], P. Verwilligen[a]

INFN Sezione di Bologna[a], Università di Bologna[b], Bologna, Italy
G. Abbiendi[a], C. Battilana[a,b], D. Bonacorsi[a,b], L. Borgonovi[a], L. Brigliadori[a], R. Campanini[a,b], P. Capiluppi[a,b], A. Castro[a,b], F.R. Cavallo[a], M. Cuffiani[a,b], G.M. Dallavalle[a], T. Diotalevi[a,b], F. Fabbri[a], A. Fanfani[a,b], P. Giacomelli[a], L. Giommi[a,b], C. Grandi[a], L. Guiducci[a,b], S. Lo Meo[a,48], L. Lunerti[a,b],

JHEP07(2023)210

S. Marcellini[a], G. Masetti[a], F.L. Navarria[a,b], A. Perrotta[a], F. Primavera[a,b], A.M. Rossi[a,b], T. Rovelli[a,b], G.P. Siroli[a,b]

INFN Sezione di Catania[a], Università di Catania[b], Catania, Italy

S. Costa[a,b,49], A. Di Mattia[a], R. Potenza[a,b], A. Tricomi[a,b,49], C. Tuve[a,b]

INFN Sezione di Firenze[a], Università di Firenze[b], Firenze, Italy

G. Barbagli[a], G. Bardelli[a,b], B. Camaiani[a,b], A. Cassese[a], R. Ceccarelli[a,b], V. Ciulli[a,b], C. Civinini[a], R. D'Alessandro[a,b], E. Focardi[a,b], G. Latino[a,b], P. Lenzi[a,b], M. Lizzo[a,b], M. Meschini[a], S. Paoletti[a], G. Sguazzoni[a], L. Viliani[a]

INFN Laboratori Nazionali di Frascati, Frascati, Italy

L. Benussi, S. Bianco, S. Meola[50], D. Piccolo

INFN Sezione di Genova[a], Università di Genova[b], Genova, Italy

M. Bozzo[a,b], P. Chatagnon[a], F. Ferro[a], E. Robutti[a], S. Tosi[a,b]

INFN Sezione di Milano-Bicocca[a], Università di Milano-Bicocca[b], Milano, Italy

A. Benaglia[a], G. Boldrini[a], F. Brivio[a,b], F. Cetorelli[a,b], F. De Guio[a,b], M.E. Dinardo[a,b], P. Dini[a], S. Gennai[a], A. Ghezzi[a,b], P. Govoni[a,b], L. Guzzi[a,b], M.T. Lucchini[a,b], M. Malberti[a], S. Malvezzi[a], A. Massironi[a], D. Menasce[a], L. Moroni[a], M. Paganoni[a,b], D. Pedrini[a], B.S. Pinolini[a], S. Ragazzi[a,b], N. Redaelli[a], T. Tabarelli de Fatis[a,b], D. Zuolo[a,b]

INFN Sezione di Napoli[a], Università di Napoli 'Federico II'[b], Napoli, Italy; Università della Basilicata[c], Potenza, Italy; Università G. Marconi[d], Roma, Italy

S. Buontempo[a], F. Carnevali[a,b], N. Cavallo[a,c], A. De Iorio[a,b], F. Fabozzi[a,c], A.O.M. Iorio[a,b], L. Lista[a,b,51], P. Paolucci[a,27], B. Rossi[a], C. Sciacca[a,b]

INFN Sezione di Padova[a], Università di Padova[b], Padova, Italy; Università di Trento[c], Trento, Italy

P. Azzi[a], N. Bacchetta[a,52], A. Bergnoli[a], D. Bisello[a,b], P. Bortignon[a], A. Bragagnolo[a,b], R. Carlin[a,b], P. Checchia[a], T. Dorigo[a], F. Gasparini[a,b], U. Gasparini[a,b], G. Grosso[a], L. Layer[a,53], E. Lusiani[a], M. Margoni[a,b], A.T. Meneguzzo[a,b], J. Pazzini[a,b], P. Ronchese[a,b], R. Rossin[a,b], F. Simonetto[a,b], G. Strong[a], M. Tosi[a,b], H. Yarar[a,b], M. Zanetti[a,b], P. Zotto[a,b], A. Zucchetta[a,b]

INFN Sezione di Pavia[a], Università di Pavia[b], Pavia, Italy

S. Abu Zeid[a,54], C. Aimè[a,b], A. Braghieri[a], S. Calzaferri[a,b], D. Fiorina[a,b], P. Montagna[a,b], V. Re[a], C. Riccardi[a,b], P. Salvini[a], I. Vai[a], P. Vitulo[a,b]

INFN Sezione di Perugia[a], Università di Perugia[b], Perugia, Italy

P. Asenov[a,55], G.M. Bilei[a], D. Ciangottini[a,b], L. Fanò[a,b], M. Magherini[a,b], G. Mantovani[a,b], V. Mariani[a,b], M. Menichelli[a], F. Moscatelli[a,55], A. Piccinelli[a,b], M. Presilla[a,b], A. Rossi[a,b], A. Santocchia[a,b], D. Spiga[a], T. Tedeschi[a,b]

JHEP07(2023)210

INFN Sezione di Pisa[a], Università di Pisa[b], Scuola Normale Superiore di Pisa[c], Pisa, Italy; Università di Siena[d], Siena, Italy

P. Azzurri[a], G. Bagliesi[a], V. Bertacchi[a,c], R. Bhattacharya[a], L. Bianchini[a,b], T. Boccali[a], E. Bossini[a,b], D. Bruschini[a,c], R. Castaldi[a], M.A. Ciocci[a,b], V. D'Amante[a,d], R. Dell'Orso[a], S. Donato[a], A. Giassi[a], F. Ligabue[a,c], D. Matos Figueiredo[a], A. Messineo[a,b], M. Musich[a,b], F. Palla[a], S. Parolia[a], G. Ramirez-Sanchez[a,c], A. Rizzi[a,b], G. Rolandi[a,c], S. Roy Chowdhury[a], T. Sarkar[a], A. Scribano[a], P. Spagnolo[a], R. Tenchini[a], G. Tonelli[a,b], N. Turini[a,d], A. Venturi[a], P.G. Verdini[a]

INFN Sezione di Roma[a], Sapienza Università di Roma[b], Roma, Italy

P. Barria[a], M. Campana[a,b], F. Cavallari[a], D. Del Re[a,b], E. Di Marco[a], M. Diemoz[a], E. Longo[a,b], P. Meridiani[a], G. Organtini[a,b], F. Pandolfi[a], R. Paramatti[a,b], C. Quaranta[a,b], S. Rahatlou[a,b], C. Rovelli[a], F. Santanastasio[a,b], L. Soffi[a], R. Tramontano[a,b]

INFN Sezione di Torino[a], Università di Torino[b], Torino, Italy; Università del Piemonte Orientale[c], Novara, Italy

N. Amapane[a,b], R. Arcidiacono[a,c], S. Argiro[a,b], M. Arneodo[a,c], N. Bartosik[a], R. Bellan[a,b], A. Bellora[a,b], C. Biino[a], N. Cartiglia[a], M. Costa[a,b], R. Covarelli[a,b], N. Demaria[a], M. Grippo[a,b], B. Kiani[a,b], F. Legger[a], C. Mariotti[a], S. Maselli[a], A. Mecca[a,b], E. Migliore[a,b], M. Monteno[a], R. Mulargia[a], M.M. Obertino[a,b], G. Ortona[a], L. Pacher[a,b], N. Pastrone[a], M. Pelliccioni[a], M. Ruspa[a,c], K. Shchelina[a], F. Siviero[a,b], V. Sola[a,b], A. Solano[a,b], D. Soldi[a,b], A. Staiano[a], M. Tornago[a,b], D. Trocino[a], G. Umoret[a,b], A. Vagnerini[a,b], E. Vlasov[a,b]

INFN Sezione di Trieste[a], Università di Trieste[b], Trieste, Italy

S. Belforte[a], V. Candelise[a,b], M. Casarsa[a], F. Cossutti[a], G. Della Ricca[a,b], G. Sorrentino[a,b]

Kyungpook National University, Daegu, Korea

S. Dogra, C. Huh, B. Kim, D.H. Kim, G.N. Kim, J. Kim, J. Lee, S.W. Lee, C.S. Moon, Y.D. Oh, S.I. Pak, M.S. Ryu, S. Sekmen, Y.C. Yang

Chonnam National University, Institute for Universe and Elementary Particles, Kwangju, Korea

H. Kim, D.H. Moon

Hanyang University, Seoul, Korea

E. Asilar, T.J. Kim, J. Park

Korea University, Seoul, Korea

S. Choi, S. Han, B. Hong, K. Lee, K.S. Lee, J. Lim, J. Park, S.K. Park, J. Yoo

JHEP07(2023)210

Kyung Hee University, Department of Physics, Seoul, Korea
J. Goh

Sejong University, Seoul, Korea
H. S. Kim, Y. Kim, S. Lee

Seoul National University, Seoul, Korea
J. Almond, J.H. Bhyun, J. Choi, S. Jeon, J. Kim, J.S. Kim, S. Ko, H. Kwon, H. Lee, S. Lee, B.H. Oh, S.B. Oh, H. Seo, U.K. Yang, I. Yoon

University of Seoul, Seoul, Korea
W. Jang, D.Y. Kang, Y. Kang, D. Kim, S. Kim, B. Ko, J.S.H. Lee, Y. Lee, J.A. Merlin, I.C. Park, Y. Roh, D. Song, I.J. Watson, S. Yang

Yonsei University, Department of Physics, Seoul, Korea
S. Ha, H.D. Yoo

Sungkyunkwan University, Suwon, Korea
M. Choi, M.R. Kim, H. Lee, Y. Lee, I. Yu

College of Engineering and Technology, American University of the Middle East (AUM), Dasman, Kuwait
T. Beyrouthy, Y. Maghrbi

Riga Technical University, Riga, Latvia
K. Dreimanis, G. Pikurs, A. Potrebko, M. Seidel, V. Veckalns

Vilnius University, Vilnius, Lithuania
M. Ambrozas, A. Carvalho Antunes De Oliveira, A. Juodagalvis, A. Rinkevicius, G. Tamulaitis

National Centre for Particle Physics, Universiti Malaya, Kuala Lumpur, Malaysia
N. Bin Norjoharuddeen, S.Y. Hoh[56], I. Yusuff[56], Z. Zolkapli

Universidad de Sonora (UNISON), Hermosillo, Mexico
J.F. Benitez, A. Castaneda Hernandez, H.A. Encinas Acosta, L.G. Gallegos Maríñez, M. León Coello, J.A. Murillo Quijada, A. Sehrawat, L. Valencia Palomo

Centro de Investigacion y de Estudios Avanzados del IPN, Mexico City, Mexico
G. Ayala, H. Castilla-Valdez, I. Heredia-De La Cruz[57], R. Lopez-Fernandez, C.A. Mondragon Herrera, D.A. Perez Navarro, A. Sánchez Hernández

Universidad Iberoamericana, Mexico City, Mexico
C. Oropeza Barrera, F. Vazquez Valencia

JHEP07(2023)210

Benemerita Universidad Autonoma de Puebla, Puebla, Mexico
I. Pedraza, H.A. Salazar Ibarguen, C. Uribe Estrada

University of Montenegro, Podgorica, Montenegro
I. Bubanja, J. Mijuskovic[58], N. Raicevic

National Centre for Physics, Quaid-I-Azam University, Islamabad, Pakistan
A. Ahmad, M.I. Asghar, A. Awais, M.I.M. Awan, M. Gul, H.R. Hoorani, W.A. Khan

AGH University of Science and Technology Faculty of Computer Science, Electronics and Telecommunications, Krakow, Poland
V. Avati, L. Grzanka, M. Malawski

National Centre for Nuclear Research, Swierk, Poland
H. Bialkowska, M. Bluj, B. Boimska, M. Górski, M. Kazana, M. Szleper, P. Zalewski

Institute of Experimental Physics, Faculty of Physics, University of Warsaw, Warsaw, Poland
K. Bunkowski, K. Doroba, A. Kalinowski, M. Konecki, J. Krolikowski

Laboratório de Instrumentação e Física Experimental de Partículas, Lisboa, Portugal
M. Araujo, P. Bargassa, D. Bastos, A. Boletti, P. Faccioli, M. Gallinaro, J. Hollar, N. Leonardo, T. Niknejad, M. Pisano, J. Seixas, J. Varela

VINCA Institute of Nuclear Sciences, University of Belgrade, Belgrade, Serbia
P. Adzic[59], M. Dordevic, P. Milenovic, J. Milosevic

Centro de Investigaciones Energéticas Medioambientales y Tecnológicas (CIEMAT), Madrid, Spain
M. Aguilar-Benitez, J. Alcaraz Maestre, M. Barrio Luna, Cristina F. Bedoya, M. Cepeda, M. Cerrada, N. Colino, B. De La Cruz, A. Delgado Peris, D. Fernández Del Val, J.P. Fernández Ramos, J. Flix, M.C. Fouz, O. Gonzalez Lopez, S. Goy Lopez, J.M. Hernandez, M.I. Josa, J. León Holgado, D. Moran, C. Perez Dengra, A. Pérez-Calero Yzquierdo, J. Puerta Pelayo, I. Redondo, D.D. Redondo Ferrero, L. Romero, S. Sánchez Navas, J. Sastre, L. Urda Gómez, J. Vazquez Escobar, C. Willmott

Universidad Autónoma de Madrid, Madrid, Spain
J.F. de Trocóniz

JHEP07(2023)210

Universidad de Oviedo, Instituto Universitario de Ciencias y Tecnologías Espaciales de Asturias (ICTEA), Oviedo, Spain

B. Alvarez Gonzalez, J. Cuevas, J. Fernandez Menendez, S. Folgueras, I. Gonzalez Caballero, J.R. González Fernández, E. Palencia Cortezon, C. Ramón Álvarez, V. Rodríguez Bouza, A. Soto Rodríguez, A. Trapote, C. Vico Villalba

Instituto de Física de Cantabria (IFCA), CSIC-Universidad de Cantabria, Santander, Spain

J.A. Brochero Cifuentes, I.J. Cabrillo, A. Calderon, J. Duarte Campderros, M. Fernandez, C. Fernandez Madrazo, A. García Alonso, G. Gomez, C. Lasaosa García, C. Martinez Rivero, P. Martinez Ruiz del Arbol, F. Matorras, P. Matorras Cuevas, J. Piedra Gomez, C. Prieels, L. Scodellaro, I. Vila, J.M. Vizan Garcia

University of Colombo, Colombo, Sri Lanka

M.K. Jayananda, B. Kailasapathy[60], D.U.J. Sonnadara, D.D.C. Wickramarathna

University of Ruhuna, Department of Physics, Matara, Sri Lanka

W.G.D. Dharmaratna, K. Liyanage, N. Perera, N. Wickramage

CERN, European Organization for Nuclear Research, Geneva, Switzerland

D. Abbaneo, E. Auffray, G. Auzinger, J. Baechler, P. Baillon[†], D. Barney, J. Bendavid, M. Bianco, B. Bilin, A.A. Bin Anuar, A. Bocci, E. Brondolin, C. Caillol, T. Camporesi, G. Cerminara, N. Chernyavskaya, S.S. Chhibra, S. Choudhury, M. Cipriani, D. d'Enterria, A. Dabrowski, A. David, A. De Roeck, M.M. Defranchis, M. Deile, M. Dobson, M. Dünser, N. Dupont, F. Fallavollita[61], A. Florent, L. Forthomme, G. Franzoni, W. Funk, S. Ghosh, S. Giani, D. Gigi, K. Gill, F. Glege, L. Gouskos, E. Govorkova, M. Haranko, J. Hegeman, V. Innocente, T. James, P. Janot, J. Kaspar, J. Kieseler, N. Kratochwil, S. Laurila, P. Lecoq, E. Leutgeb, C. Lourenço, B. Maier, L. Malgeri, M. Mannelli, A.C. Marini, F. Meijers, S. Mersi, E. Meschi, F. Moortgat, M. Mulders, S. Orfanelli, L. Orsini, F. Pantaleo, E. Perez, M. Peruzzi, A. Petrilli, G. Petrucciani, A. Pfeiffer, M. Pierini, D. Piparo, M. Pitt, H. Qu, T. Quast, D. Rabady, A. Racz, G. Reales Gutiérrez, M. Rovere, H. Sakulin, J. Salfeld-Nebgen, S. Scarfi, M. Selvaggi, A. Sharma, P. Silva, P. Sphicas[62], A.G. Stahl Leiton, S. Summers, K. Tatar, D. Treille, P. Tropea, A. Tsirou, J. Wanczyk[63], K.A. Wozniak, W.D. Zeuner

Paul Scherrer Institut, Villigen, Switzerland

L. Caminada[64], A. Ebrahimi, W. Erdmann, R. Horisberger, Q. Ingram, H.C. Kaestli, D. Kotlinski, C. Lange, M. Missiroli[64], L. Noehte[64], T. Rohe

ETH Zurich — Institute for Particle Physics and Astrophysics (IPA), Zurich, Switzerland

T.K. Aarrestad, K. Androsov[63], M. Backhaus, A. Calandri, K. Datta, A. De Cosa, G. Dissertori, M. Dittmar, M. Donegà, F. Eble, M. Galli, K. Gedia, F. Glessgen,

JHEP07(2023)210

T.A. Gómez Espinosa, C. Grab, D. Hits, W. Lustermann, A.-M. Lyon, R.A. Manzoni, L. Marchese, C. Martin Perez, A. Mascellani[63], F. Nessi-Tedaldi, J. Niedziela, F. Pauss, V. Perovic, S. Pigazzini, M.G. Ratti, M. Reichmann, C. Reissel, T. Reitenspiess, B. Ristic, F. Riti, D. Ruini, D.A. Sanz Becerra, R. Seidita, J. Steggemann[63], D. Valsecchi, R. Wallny

Universität Zürich, Zurich, Switzerland

C. Amsler[65], P. Bärtschi, C. Botta, D. Brzhechko, M.F. Canelli, K. Cormier, A. De Wit, R. Del Burgo, J.K. Heikkilä, M. Huwiler, W. Jin, A. Jofrehei, B. Kilminster, S. Leontsinis, S.P. Liechti, A. Macchiolo, P. Meiring, V.M. Mikuni, U. Molinatti, I. Neutelings, A. Reimers, P. Robmann, S. Sanchez Cruz, K. Schweiger, M. Senger, Y. Takahashi

National Central University, Chung-Li, Taiwan

C. Adloff[66], C.M. Kuo, W. Lin, P.K. Rout, P.C. Tiwari[39], S.S. Yu

National Taiwan University (NTU), Taipei, Taiwan

L. Ceard, Y. Chao, K.F. Chen, P.s. Chen, H. Cheng, W.-S. Hou, R. Khurana, G. Kole, Y.y. Li, R.-S. Lu, E. Paganis, A. Psallidas, A. Steen, H.y. Wu, E. Yazgan

Chulalongkorn University, Faculty of Science, Department of Physics, Bangkok, Thailand

C. Asawatangtrakuldee, N. Srimanobhas, V. Wachirapusitanand

Çukurova University, Physics Department, Science and Art Faculty, Adana, Turkey

D. Agyel, F. Boran, Z.S. Demiroglu, F. Dolek, I. Dumanoglu[67], E. Eskut, Y. Guler[68], E. Gurpinar Guler[68], C. Isik, O. Kara, A. Kayis Topaksu, U. Kiminsu, G. Onengut, K. Ozdemir[69], A. Polatoz, A.E. Simsek, B. Tali[70], U.G. Tok, S. Turkcapar, E. Uslan, I.S. Zorbakir

Middle East Technical University, Physics Department, Ankara, Turkey

G. Karapinar[71], K. Ocalan[72], M. Yalvac[73]

Bogazici University, Istanbul, Turkey

B. Akgun, I.O. Atakisi, E. Gülmez, M. Kaya[74], O. Kaya[75], S. Tekten[76]

Istanbul Technical University, Istanbul, Turkey

A. Cakir, K. Cankocak[67], Y. Komurcu, S. Sen[77]

Istanbul University, Istanbul, Turkey

O. Aydilek, S. Cerci[70], B. Hacisahinoglu, I. Hos[78], B. Isildak[79], B. Kaynak, S. Ozkorucuklu, C. Simsek, D. Sunar Cerci[70]

JHEP07(2023)210

Institute for Scintillation Materials of National Academy of Science of Ukraine, Kharkiv, Ukraine

B. Grynyov

National Science Centre, Kharkiv Institute of Physics and Technology, Kharkiv, Ukraine

L. Levchuk

University of Bristol, Bristol, United Kingdom

D. Anthony, J.J. Brooke, A. Bundock, E. Clement, D. Cussans, H. Flacher, M. Glowacki, J. Goldstein, H.F. Heath, L. Kreczko, B. Krikler, S. Paramesvaran, S. Seif El Nasr-Storey, V.J. Smith, N. Stylianou[80], K. Walkingshaw Pass, R. White

Rutherford Appleton Laboratory, Didcot, United Kingdom

A.H. Ball, K.W. Bell, A. Belyaev[81], C. Brew, R.M. Brown, D.J.A. Cockerill, C. Cooke, K.V. Ellis, K. Harder, S. Harper, M.-L. Holmberg[82], Sh. Jain, J. Linacre, K. Manolopoulos, D.M. Newbold, E. Olaiya, D. Petyt, T. Reis, G. Salvi, T. Schuh, C.H. Shepherd-Themistocleous, I.R. Tomalin, T. Williams

Imperial College, London, United Kingdom

R. Bainbridge, P. Bloch, S. Bonomally, J. Borg, C.E. Brown, O. Buchmuller, V. Cacchio, C.A. Carrillo Montoya, V. Cepaitis, G.S. Chahal[83], D. Colling, J.S. Dancu, P. Dauncey, G. Davies, J. Davies, M. Della Negra, S. Fayer, G. Fedi, G. Hall, M.H. Hassanshahi, A. Howard, G. Iles, J. Langford, L. Lyons, A.-M. Magnan, S. Malik, A. Martelli, M. Mieskolainen, D.G. Monk, J. Nash[84], M. Pesaresi, B.C. Radburn-Smith, D.M. Raymond, A. Richards, A. Rose, E. Scott, C. Seez, R. Shukla, A. Tapper, K. Uchida, G.P. Uttley, L.H. Vage, T. Virdee[27], M. Vojinovic, N. Wardle, S.N. Webb, D. Winterbottom

Brunel University, Uxbridge, United Kingdom

K. Coldham, J.E. Cole, A. Khan, P. Kyberd, I.D. Reid

Baylor University, Waco, Texas, U.S.A.

S. Abdullin, A. Brinkerhoff, B. Caraway, J. Dittmann, K. Hatakeyama, A.R. Kanuganti, B. McMaster, M. Saunders, S. Sawant, C. Sutantawibul, M. Toms, J. Wilson

Catholic University of America, Washington, DC, U.S.A.

R. Bartek, A. Dominguez, C. Huerta Escamilla, R. Uniyal, A.M. Vargas Hernandez

The University of Alabama, Tuscaloosa, Alabama, U.S.A.

R. Chudasama, S.I. Cooper, D. Di Croce, S.V. Gleyzer, C. Henderson, C.U. Perez, P. Rumerio[85], C. West

JHEP07(2023)210

Boston University, Boston, Massachusetts, U.S.A.

A. Akpinar, A. Albert, D. Arcaro, C. Cosby, Z. Demiragli, C. Erice, E. Fontanesi, D. Gastler, S. May, J. Rohlf, K. Salyer, D. Sperka, D. Spitzbart, I. Suarez, A. Tsatsos, S. Yuan

Brown University, Providence, Rhode Island, U.S.A.

G. Benelli, B. Burkle, X. Coubez[22], D. Cutts, M. Hadley, U. Heintz, J.M. Hogan[86], T. Kwon, G. Landsberg, K.T. Lau, D. Li, J. Luo, M. Narain, N. Pervan, S. Sagir[87], F. Simpson, E. Usai, W.Y. Wong, X. Yan, D. Yu, W. Zhang

University of California, Davis, Davis, California, U.S.A.

S. Abbott, J. Bonilla, C. Brainerd, R. Breedon, M. Calderon De La Barca Sanchez, M. Chertok, J. Conway, P.T. Cox, R. Erbacher, G. Haza, F. Jensen, O. Kukral, G. Mocellin, M. Mulhearn, D. Pellett, B. Regnery, Y. Yao, F. Zhang

University of California, Los Angeles, California, U.S.A.

M. Bachtis, R. Cousins, A. Datta, J. Hauser, M. Ignatenko, M.A. Iqbal, T. Lam, E. Manca, W.A. Nash, D. Saltzberg, B. Stone, V. Valuev

University of California, Riverside, Riverside, California, U.S.A.

R. Clare, J.W. Gary, M. Gordon, G. Hanson, O.R. Long, N. Manganelli, W. Si, S. Wimpenny

University of California, San Diego, La Jolla, California, U.S.A.

J.G. Branson, S. Cittolin, S. Cooperstein, D. Diaz, J. Duarte, R. Gerosa, L. Giannini, J. Guiang, R. Kansal, V. Krutelyov, R. Lee, J. Letts, M. Masciovecchio, F. Mokhtar, M. Pieri, M. Quinnan, B.V. Sathia Narayanan, V. Sharma, M. Tadel, E. Vourliotis, F. Würthwein, Y. Xiang, A. Yagil

University of California, Santa Barbara — Department of Physics, Santa Barbara, California, U.S.A.

N. Amin, C. Campagnari, M. Citron, G. Collura, A. Dorsett, J. Incandela, M. Kilpatrick, J. Kim, A.J. Li, P. Masterson, H. Mei, M. Oshiro, J. Richman, U. Sarica, R. Schmitz, F. Setti, J. Sheplock, P. Siddireddy, D. Stuart, S. Wang

California Institute of Technology, Pasadena, California, U.S.A.

A. Bornheim, O. Cerri, I. Dutta, A. Latorre, J.M. Lawhorn, J. Mao, H.B. Newman, T. Q. Nguyen, M. Spiropulu, J.R. Vlimant, C. Wang, S. Xie, R.Y. Zhu

Carnegie Mellon University, Pittsburgh, Pennsylvania, U.S.A.

J. Alison, S. An, M.B. Andrews, P. Bryant, V. Dutta, T. Ferguson, A. Harilal, C. Liu, T. Mudholkar, S. Murthy, M. Paulini, A. Roberts, A. Sanchez, W. Terrill

JHEP07(2023)210

University of Colorado Boulder, Boulder, Colorado, U.S.A.

J.P. Cumalat, W.T. Ford, A. Hassani, G. Karathanasis, E. MacDonald, F. Marini, A. Perloff, C. Savard, N. Schonbeck, K. Stenson, K.A. Ulmer, S.R. Wagner, N. Zipper

Cornell University, Ithaca, New York, U.S.A.

J. Alexander, S. Bright-Thonney, X. Chen, D.J. Cranshaw, J. Fan, X. Fan, D. Gadkari, S. Hogan, J. Monroy, J.R. Patterson, J. Reichert, M. Reid, A. Ryd, J. Thom, P. Wittich, R. Zou

Fermi National Accelerator Laboratory, Batavia, Illinois, U.S.A.

M. Albrow, M. Alyari, G. Apollinari, A. Apresyan, L.A.T. Bauerdick, D. Berry, J. Berryhill, P.C. Bhat, K. Burkett, J.N. Butler, A. Canepa, G.B. Cerati, H.W.K. Cheung, F. Chlebana, K.F. Di Petrillo, J. Dickinson, V.D. Elvira, Y. Feng, J. Freeman, A. Gandrakota, Z. Gecse, L. Gray, D. Green, S. Grünendahl, D. Guerrero, O. Gutsche, R.M. Harris, R. Heller, T.C. Herwig, J. Hirschauer, L. Horyn, B. Jayatilaka, S. Jindariani, M. Johnson, U. Joshi, T. Klijnsma, B. Klima, K.H.M. Kwok, S. Lammel, D. Lincoln, R. Lipton, T. Liu, C. Madrid, K. Maeshima, C. Mantilla, D. Mason, P. McBride, P. Merkel, S. Mrenna, S. Nahn, J. Ngadiuba, D. Noonan, S. Norberg, V. Papadimitriou, N. Pastika, K. Pedro, C. Pena[88], F. Ravera, A. Reinsvold Hall[89], L. Ristori, E. Sexton-Kennedy, N. Smith, A. Soha, L. Spiegel, J. Strait, L. Taylor, S. Tkaczyk, N.V. Tran, L. Uplegger, E.W. Vaandering, I. Zoi

University of Florida, Gainesville, Florida, U.S.A.

P. Avery, D. Bourilkov, L. Cadamuro, P. Chang, V. Cherepanov, R.D. Field, E. Koenig, M. Kolosova, J. Konigsberg, A. Korytov, E. Kuznetsova, K.H. Lo, K. Matchev, N. Menendez, G. Mitselmakher, A. Muthirakalayil Madhu, N. Rawal, D. Rosenzweig, S. Rosenzweig, K. Shi, J. Wang, Z. Wu

Florida State University, Tallahassee, Florida, U.S.A.

T. Adams, A. Askew, N. Bower, R. Habibullah, V. Hagopian, T. Kolberg, G. Martinez, H. Prosper, O. Viazlo, M. Wulansatiti, R. Yohay, J. Zhang

Florida Institute of Technology, Melbourne, Florida, U.S.A.

M.M. Baarmand, S. Butalla, T. Elkafrawy[54], M. Hohlmann, R. Kumar Verma, M. Rahmani, F. Yumiceva

University of Illinois at Chicago (UIC), Chicago, Illinois, U.S.A.

M.R. Adams, R. Cavanaugh, S. Dittmer, O. Evdokimov, C.E. Gerber, D.J. Hofman, D. S. Lemos, A.H. Merrit, C. Mills, G. Oh, T. Roy, S. Rudrabhatla, M.B. Tonjes, N. Varelas, X. Wang, Z. Ye, J. Yoo

JHEP07(2023)210

The University of Iowa, Iowa City, Iowa, U.S.A.
M. Alhusseini, K. Dilsiz[90], L. Emediato, G. Karaman, O.K. Köseyan, J.-P. Merlo, A. Mestvirishvili[91], J. Nachtman, O. Neogi, H. Ogul[92], Y. Onel, A. Penzo, C. Snyder, E. Tiras[93]

Johns Hopkins University, Baltimore, Maryland, U.S.A.
O. Amram, B. Blumenfeld, L. Corcodilos, J. Davis, A.V. Gritsan, S. Kyriacou, P. Maksimovic, J. Roskes, S. Sekhar, M. Swartz, T.Á. Vámi

The University of Kansas, Lawrence, Kansas, U.S.A.
A. Abreu, L.F. Alcerro Alcerro, J. Anguiano, P. Baringer, A. Bean, Z. Flowers, J. King, G. Krintiras, M. Lazarovits, C. Le Mahieu, C. Lindsey, J. Marquez, N. Minafra, M. Murray, M. Nickel, C. Rogan, C. Royon, R. Salvatico, S. Sanders, C. Smith, Q. Wang, G. Wilson

Kansas State University, Manhattan, Kansas, U.S.A.
B. Allmond, S. Duric, A. Ivanov, K. Kaadze, A. Kalogeropoulos, D. Kim, Y. Maravin, T. Mitchell, A. Modak, K. Nam, D. Roy

Lawrence Livermore National Laboratory, Livermore, California, U.S.A.
F. Rebassoo, D. Wright

University of Maryland, College Park, Maryland, U.S.A.
E. Adams, A. Baden, O. Baron, A. Belloni, A. Bethani, S.C. Eno, N.J. Hadley, S. Jabeen, R.G. Kellogg, T. Koeth, Y. Lai, S. Lascio, A.C. Mignerey, S. Nabili, C. Palmer, C. Papageorgakis, L. Wang, K. Wong

Massachusetts Institute of Technology, Cambridge, Massachusetts, U.S.A.
W. Busza, I.A. Cali, Y. Chen, M. D'Alfonso, J. Eysermans, C. Freer, G. Gomez-Ceballos, M. Goncharov, P. Harris, M. Hu, D. Kovalskyi, J. Krupa, Y.-J. Lee, K. Long, C. Mironov, C. Paus, D. Rankin, C. Roland, G. Roland, Z. Shi, G.S.F. Stephans, J. Wang, Z. Wang, B. Wyslouch, T. J. Yang

University of Minnesota, Minneapolis, Minnesota, U.S.A.
R.M. Chatterjee, B. Crossman, J. Hiltbrand, B.M. Joshi, C. Kapsiak, M. Krohn, Y. Kubota, D. Mahon, J. Mans, M. Revering, R. Rusack, R. Saradhy, N. Schroeder, N. Strobbe, M.A. Wadud

University of Mississippi, Oxford, Mississippi, U.S.A.
L.M. Cremaldi

University of Nebraska-Lincoln, Lincoln, Nebraska, U.S.A.
K. Bloom, M. Bryson, D.R. Claes, C. Fangmeier, L. Finco, F. Golf, C. Joo, R. Kamalieddin, I. Kravchenko, I. Reed, J.E. Siado, G.R. Snow[†], W. Tabb, A. Wightman, F. Yan, A.G. Zecchinelli

JHEP07(2023)210

State University of New York at Buffalo, Buffalo, New York, U.S.A.
G. Agarwal, H. Bandyopadhyay, L. Hay, I. Iashvili, A. Kharchilava, C. McLean, M. Morris, D. Nguyen, J. Pekkanen, S. Rappoccio, A. Williams

Northeastern University, Boston, Massachusetts, U.S.A.
G. Alverson, E. Barberis, Y. Haddad, Y. Han, A. Krishna, J. Li, J. Lidrych, G. Madigan, B. Marzocchi, D.M. Morse, V. Nguyen, T. Orimoto, A. Parker, L. Skinnari, A. Tishelman-Charny, T. Wamorkar, B. Wang, A. Wisecarver, D. Wood

Northwestern University, Evanston, Illinois, U.S.A.
S. Bhattacharya, J. Bueghly, Z. Chen, A. Gilbert, K.A. Hahn, Y. Liu, N. Odell, M.H. Schmitt, M. Velasco

University of Notre Dame, Notre Dame, Indiana, U.S.A.
R. Band, R. Bucci, M. Cremonesi, A. Das, R. Goldouzian, M. Hildreth, K. Hurtado Anampa, C. Jessop, K. Lannon, J. Lawrence, N. Loukas, L. Lutton, J. Mariano, N. Marinelli, I. Mcalister, T. McCauley, C. Mcgrady, K. Mohrman, C. Moore, Y. Musienko[12], R. Ruchti, A. Townsend, M. Wayne, H. Yockey, M. Zarucki, L. Zygala

The Ohio State University, Columbus, Ohio, U.S.A.
B. Bylsma, M. Carrigan, L.S. Durkin, C. Hill, M. Joyce, A. Lesauvage, M. Nunez Ornelas, K. Wei, B.L. Winer, B. R. Yates

Princeton University, Princeton, New Jersey, U.S.A.
F.M. Addesa, P. Das, G. Dezoort, P. Elmer, A. Frankenthal, B. Greenberg, N. Haubrich, S. Higginbotham, G. Kopp, S. Kwan, D. Lange, A. Loeliger, D. Marlow, I. Ojalvo, J. Olsen, D. Stickland, C. Tully

University of Puerto Rico, Mayaguez, Puerto Rico, U.S.A.
S. Malik

Purdue University, West Lafayette, Indiana, U.S.A.
A.S. Bakshi, V.E. Barnes, R. Chawla, S. Das, L. Gutay, M. Jones, A.W. Jung, D. Kondratyev, A.M. Koshy, M. Liu, G. Negro, N. Neumeister, G. Paspalaki, S. Piperov, A. Purohit, J.F. Schulte, M. Stojanovic, J. Thieman, F. Wang, R. Xiao, W. Xie

Purdue University Northwest, Hammond, Indiana, U.S.A.
J. Dolen, N. Parashar

Rice University, Houston, Texas, U.S.A.
D. Acosta, A. Baty, T. Carnahan, S. Dildick, K.M. Ecklund, P.J. Fernández Manteca, S. Freed, P. Gardner, F.J.M. Geurts, A. Kumar, W. Li, B.P. Padley, R. Redjimi, J. Rotter, S. Yang, E. Yigitbasi, Y. Zhang

JHEP07(2023)210

University of Rochester, Rochester, New York, U.S.A.
A. Bodek, P. de Barbaro, R. Demina, J.L. Dulemba, C. Fallon, A. Garcia-Bellido, O. Hindrichs, A. Khukhunaishvili, P. Parygin, E. Popova, R. Taus, G.P. Van Onsem

The Rockefeller University, New York, New York, U.S.A.
K. Goulianos

Rutgers, The State University of New Jersey, Piscataway, New Jersey, U.S.A.
B. Chiarito, J.P. Chou, Y. Gershtein, E. Halkiadakis, A. Hart, M. Heindl, D. Jaroslawski, O. Karacheban[25], I. Laflotte, A. Lath, R. Montalvo, K. Nash, M. Osherson, H. Routray, S. Salur, S. Schnetzer, S. Somalwar, R. Stone, S.A. Thayil, S. Thomas, H. Wang

University of Tennessee, Knoxville, Tennessee, U.S.A.
H. Acharya, A.G. Delannoy, S. Fiorendi, T. Holmes, E. Nibigira, S. Spanier

Texas A&M University, College Station, Texas, U.S.A.
O. Bouhali[94], M. Dalchenko, A. Delgado, R. Eusebi, J. Gilmore, T. Huang, T. Kamon[95], H. Kim, S. Luo, S. Malhotra, R. Mueller, D. Overton, D. Rathjens, A. Safonov

Texas Tech University, Lubbock, Texas, U.S.A.
N. Akchurin, J. Damgov, V. Hegde, K. Lamichhane, S.W. Lee, T. Mengke, S. Muthumuni, T. Peltola, I. Volobouev, A. Whitbeck

Vanderbilt University, Nashville, Tennessee, U.S.A.
E. Appelt, S. Greene, A. Gurrola, W. Johns, A. Melo, F. Romeo, P. Sheldon, S. Tuo, J. Velkovska, J. Viinikainen

University of Virginia, Charlottesville, Virginia, U.S.A.
B. Cardwell, B. Cox, G. Cummings, J. Hakala, R. Hirosky, A. Ledovskoy, A. Li, C. Neu, C.E. Perez Lara

Wayne State University, Detroit, Michigan, U.S.A.
P.E. Karchin

University of Wisconsin — Madison, Madison, Wisconsin, U.S.A.
A. Aravind, S. Banerjee, K. Black, T. Bose, S. Dasu, I. De Bruyn, P. Everaerts, C. Galloni, H. He, M. Herndon, A. Herve, C.K. Koraka, A. Lanaro, R. Loveless, J. Madhusudanan Sreekala, A. Mallampalli, A. Mohammadi, S. Mondal, G. Parida, D. Pinna, A. Savin, V. Shang, V. Sharma, W.H. Smith, D. Teague, H.F. Tsoi, W. Vetens, A. Warden

JHEP07(2023)210

Authors affiliated with an institute or an international laboratory covered by a cooperation agreement with CERN

S. Afanasiev, V. Andreev, Yu. Andreev, T. Aushev, M. Azarkin, A. Babaev, A. Belyaev, V. Blinov[96], E. Boos, V. Borshch, D. Budkouski, V. Bunichev, M. Chadeeva[96], V. Chekhovsky, R. Chistov[96], A. Dermenev, T. Dimova[96], I. Dremin, M. Dubinin[88], L. Dudko, V. Epshteyn, A. Ershov, G. Gavrilov, V. Gavrilov, S. Gninenko, V. Golovtcov, N. Golubev, I. Golutvin, I. Gorbunov, A. Gribushin, Y. Ivanov, V. Kachanov, L. Kardapoltsev[96], V. Karjavine, A. Karneyeu, V. Kim[96], M. Kirakosyan, D. Kirpichnikov, M. Kirsanov, V. Klyukhin, O. Kodolova[97], D. Konstantinov, V. Korenkov, A. Kozyrev[96], N. Krasnikov, A. Lanev, P. Levchenko, A. Litomin, N. Lychkovskaya, V. Makarenko, A. Malakhov, V. Matveev[96], V. Murzin, A. Nikitenko[98], S. Obraztsov, A. Oskin, I. Ovtin[96], V. Palichik, V. Perelygin, S. Polikarpov[96], V. Popov, O. Radchenko[96], M. Savina, V. Savrin, V. Shalaev, S. Shmatov, S. Shulha, Y. Skovpen[96], S. Slabospitskii, V. Smirnov, A. Snigirev, D. Sosnov, V. Sulimov, E. Tcherniaev, A. Terkulov, O. Teryaev, I. Tlisova, A. Toropin, L. Uvarov, A. Uzunian, A. Vorobyev[†], N. Voytishin, B.S. Yuldashev[99], A. Zarubin, I. Zhizhin, A. Zhokin

[†] *Deceased*
[1] *Also at Yerevan State University, Yerevan, Armenia*
[2] *Also at TU Wien, Vienna, Austria*
[3] *Also at Institute of Basic and Applied Sciences, Faculty of Engineering, Arab Academy for Science, Technology and Maritime Transport, Alexandria, Egypt*
[4] *Also at Université Libre de Bruxelles, Bruxelles, Belgium*
[5] *Also at Universidade Estadual de Campinas, Campinas, Brazil*
[6] *Also at Federal University of Rio Grande do Sul, Porto Alegre, Brazil*
[7] *Also at UFMS, Nova Andradina, Brazil*
[8] *Also at University of Chinese Academy of Sciences, Beijing, China*
[9] *Also at Nanjing Normal University Department of Physics, Nanjing, China*
[10] *Now at The University of Iowa, Iowa City, Iowa, U.S.A.*
[11] *Also at University of Chinese Academy of Sciences, Beijing, China*
[12] *Also at an institute or an international laboratory covered by a cooperation agreement with CERN*
[13] *Also at Cairo University, Cairo, Egypt*
[14] *Also at Suez University, Suez, Egypt*
[15] *Now at British University in Egypt, Cairo, Egypt*
[16] *Also at Purdue University, West Lafayette, Indiana, U.S.A.*
[17] *Also at Université de Haute Alsace, Mulhouse, France*
[18] *Also at Department of Physics, Tsinghua University, Beijing, China*
[19] *Also at The University of the State of Amazonas, Manaus, Brazil*
[20] *Also at Erzincan Binali Yildirim University, Erzincan, Turkey*
[21] *Also at University of Hamburg, Hamburg, Germany*
[22] *Also at RWTH Aachen University, III. Physikalisches Institut A, Aachen, Germany*
[23] *Also at Isfahan University of Technology, Isfahan, Iran*
[24] *Also at Bergische University Wuppertal (BUW), Wuppertal, Germany*
[25] *Also at Brandenburg University of Technology, Cottbus, Germany*
[26] *Also at Forschungszentrum Jülich, Juelich, Germany*
[27] *Also at CERN, European Organization for Nuclear Research, Geneva, Switzerland*
[28] *Also at Physics Department, Faculty of Science, Assiut University, Assiut, Egypt*
[29] *Also at Karoly Robert Campus, MATE Institute of Technology, Gyongyos, Hungary*

JHEP07(2023)210

[30] Also at Wigner Research Centre for Physics, Budapest, Hungary
[31] Also at Institute of Physics, University of Debrecen, Debrecen, Hungary
[32] Also at Institute of Nuclear Research ATOMKI, Debrecen, Hungary
[33] Now at Universitatea Babes-Bolyai — Facultatea de Fizica, Cluj-Napoca, Romania
[34] Also at Faculty of Informatics, University of Debrecen, Debrecen, Hungary
[35] Also at Punjab Agricultural University, Ludhiana, India
[36] Also at UPES — University of Petroleum and Energy Studies, Dehradun, India
[37] Also at University of Visva-Bharati, Santiniketan, India
[38] Also at University of Hyderabad, Hyderabad, India
[39] Also at Indian Institute of Science (IISc), Bangalore, India
[40] Also at Indian Institute of Technology (IIT), Mumbai, India
[41] Also at IIT Bhubaneswar, Bhubaneswar, India
[42] Also at Institute of Physics, Bhubaneswar, India
[43] Also at Deutsches Elektronen-Synchrotron, Hamburg, Germany
[44] Now at Department of Physics, Isfahan University of Technology, Isfahan, Iran
[45] Also at Sharif University of Technology, Tehran, Iran
[46] Also at Department of Physics, University of Science and Technology of Mazandaran, Behshahr, Iran
[47] Also at Helwan University, Cairo, Egypt
[48] Also at Italian National Agency for New Technologies, Energy and Sustainable Economic Development, Bologna, Italy
[49] Also at Centro Siciliano di Fisica Nucleare e di Struttura Della Materia, Catania, Italy
[50] Also at Università degli Studi Guglielmo Marconi, Roma, Italy
[51] Also at Scuola Superiore Meridionale, Università di Napoli 'Federico II', Napoli, Italy
[52] Also at Fermi National Accelerator Laboratory, Batavia, Illinois, U.S.A.
[53] Also at Università di Napoli 'Federico II', Napoli, Italy
[54] Also at Ain Shams University, Cairo, Egypt
[55] Also at Consiglio Nazionale delle Ricerche — Istituto Officina dei Materiali, Perugia, Italy
[56] Also at Department of Applied Physics, Faculty of Science and Technology, Universiti Kebangsaan Malaysia, Bangi, Malaysia
[57] Also at Consejo Nacional de Ciencia y Tecnología, Mexico City, Mexico
[58] Also at IRFU, CEA, Université Paris-Saclay, Gif-sur-Yvette, France
[59] Also at Faculty of Physics, University of Belgrade, Belgrade, Serbia
[60] Also at Trincomalee Campus, Eastern University, Sri Lanka, Nilaveli, Sri Lanka
[61] Also at INFN Sezione di Pavia, Università di Pavia, Pavia, Italy
[62] Also at National and Kapodistrian University of Athens, Athens, Greece
[63] Also at Ecole Polytechnique Fédérale Lausanne, Lausanne, Switzerland
[64] Also at Universität Zürich, Zurich, Switzerland
[65] Also at Stefan Meyer Institute for Subatomic Physics, Vienna, Austria
[66] Also at Laboratoire d'Annecy-le-Vieux de Physique des Particules, IN2P3-CNRS, Annecy-le-Vieux, France
[67] Also at Near East University, Research Center of Experimental Health Science, Mersin, Turkey
[68] Also at Konya Technical University, Konya, Turkey
[69] Also at Izmir Bakircay University, Izmir, Turkey
[70] Also at Adiyaman University, Adiyaman, Turkey
[71] Also at Istanbul Gedik University, Istanbul, Turkey
[72] Also at Necmettin Erbakan University, Konya, Turkey
[73] Also at Bozok Universitetesi Rektörlügü, Yozgat, Turkey
[74] Also at Marmara University, Istanbul, Turkey
[75] Also at Milli Savunma University, Istanbul, Turkey
[76] Also at Kafkas University, Kars, Turkey
[77] Also at Hacettepe University, Ankara, Turkey
[78] Also at Istanbul University — Cerrahpasa, Faculty of Engineering, Istanbul, Turkey

JHEP07(2023)210

[79] *Also at Ozyegin University, Istanbul, Turkey*
[80] *Also at Vrije Universiteit Brussel, Brussel, Belgium*
[81] *Also at School of Physics and Astronomy, University of Southampton, Southampton, United Kingdom*
[82] *Also at University of Bristol, Bristol, United Kingdom*
[83] *Also at IPPP Durham University, Durham, United Kingdom*
[84] *Also at Monash University, Faculty of Science, Clayton, Australia*
[85] *Also at Università di Torino, Torino, Italy*
[86] *Also at Bethel University, St. Paul, Minnesota, U.S.A.*
[87] *Also at Karamanoğlu Mehmetbey University, Karaman, Turkey*
[88] *Also at California Institute of Technology, Pasadena, California, U.S.A.*
[89] *Also at United States Naval Academy, Annapolis, Maryland, U.S.A.*
[90] *Also at Bingol University, Bingol, Turkey*
[91] *Also at Georgian Technical University, Tbilisi, Georgia*
[92] *Also at Sinop University, Sinop, Turkey*
[93] *Also at Erciyes University, Kayseri, Turkey*
[94] *Also at Texas A&M University at Qatar, Doha, Qatar*
[95] *Also at Kyungpook National University, Daegu, Korea*
[96] *Also at another institute or international laboratory covered by a cooperation agreement with CERN*
[97] *Also at Yerevan Physics Institute, Yerevan, Armenia*
[98] *Also at Imperial College, London, United Kingdom*
[99] *Also at Institute of Nuclear Physics of the Uzbekistan Academy of Sciences, Tashkent, Uzbekistan*

JHEP07(2023)210